Supplementary Information

Table of Contents

1. Methods & Materials

Synthesis of "ene" small molecules.

Biomass derived monomers.

While petrochemical-based polymers are the foundation of most photocured products, growing environmental and economic issues require polymers derived from renewable resources that offer competitive mechanical performance. Natural biomass resources from biological photosynthesis offer a wide variety of feedstocks for this purpose. Lignocellulosic biomass-based furfural is one such example, which can be converted into sustainably produced diacids via catalytic oxidation and easily functionalized to form monomers with terminal allylic unsaturations.

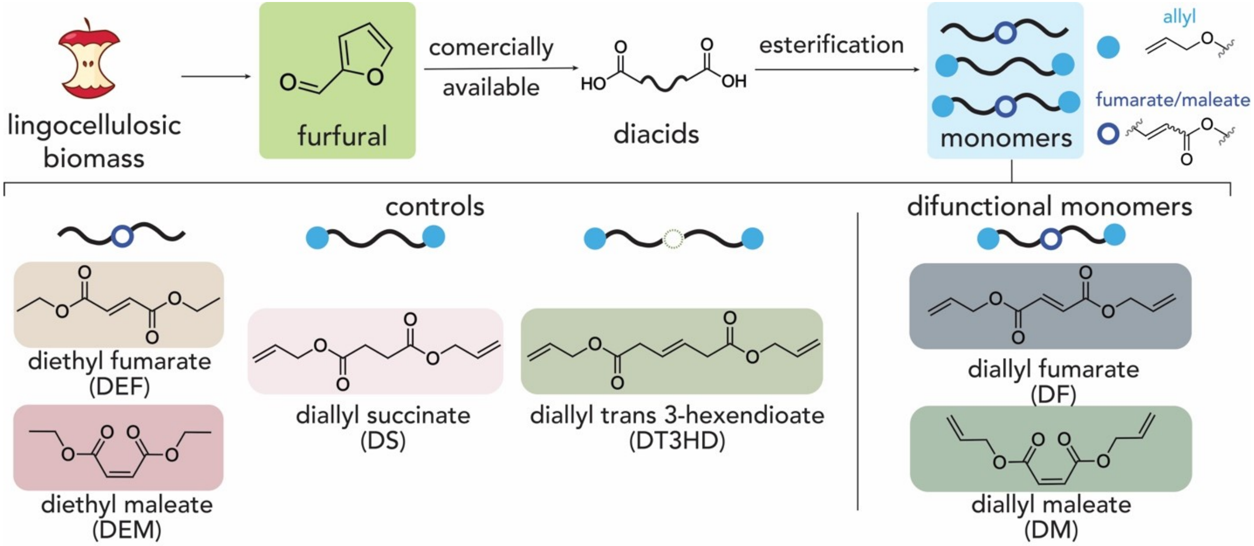

Figure S1-00: Lignocellulosic-biomass derived diacids were used to synthesize the ene-monomers for this study. For the proposed dual-crosslinking mechanism, difunctional monomers with terminal ene groups for thiol-ene click chemistry and internal unsaturations for homopolymerization were studied. Select "ene" monomers were used as controls for baseline studies.

General synthetic protocols.

Synthesis of diethyl fumarate (DEF): To a 250 mL round bottom flask equipped with a stir bar, a given diacid (1.00 equiv., 10 g, 86.1 mmol), p-toluenesulfonic acid monohydrate (0.10 equiv., 1.64 g, 8.6 mmol), and sodium sulfate (2 equiv., 1.64 g, 172 mmol) was diluted in toluene (≈ 0.5 M, 170 mL). To this stirring suspension, ethanol (10.00 equiv., 39.7 g, 861 mmol) was added. The flask was equipped with a reflux condenser and heated to 110°C in an oil bath overnight (~ 16 hours). After this period, the reaction mixture was cooled to room temperature and filtered. The filter cake was washed with toluene (10 mL, 3x) and the collected filtrate was concentrated under reduced pressure to a colorless oil. The crude product was dissolved in 200 mL of ethyl acetate, transferred to a 500 mL separatory funnel, and washed with supersaturated aqueous $NaHCO_3$ (100 mL, 2X) and brine (100 mL, 2X). After separation, organics were dried over Na_2SO_4, filtered, concentrated under reduced pressure, and dried *in vacuo* to afford a colorless, clear oil.

General Procedure for allylation of diacids[1]. To a 500 mL round bottom flask equipped with a stir bar, a given diacid (1.00 equiv, 130 mmol), p-toluenesulfonic acid monohydrate (0.10 equiv, 13 mmol), and sodium sulfate (2 equiv, 260 mmol) was diluted in toluene (≈ 0.5 M, 250 mL). To this stirring suspension, allyl alcohol (4.00 equiv, 520 mmol) was added. The flask was equipped with a reflux condenser and heated to 110°C in an oil bath overnight (~ 16 hours). After this period, the flask was cooled to room temperature and filtered and the filter cake was washed with toluene (10 mL, 3x). The filtrate was concentrated under reduced pressure to yield a yellow oil. The crude product was dissolved in 300 mL of ethyl acetate, transferred to a 1000 mL separatory funnel, and washed with supersaturated aqueous $NaHCO_3$ (150 mL, 2X) and brine (150 mL, 2X). After separation, organics were dried over Na_2SO_4, filtered, concentrated under reduced pressure, and dried *in vacuo** to afford a light yellow, clear oil. *In the case of fumaric acid, the subsequent residue was submitted to column chromatography with an 80 to 20 hexanes to ethyl acetate eluent ratio. Concentration of selected fractions yielded the clear oil product.

H^{1} and C^{13} NMR Spectra of Synthesized Compounds.

Diethyl fumarate (DEF). ^{1}H NMR (500 mHz, $CDCl_3$): 6.78 (q, J = 1.8 Hz, 1H), 4.24 – 4.15 (m, 2H), 1.29 – 1.22 (m, 3H). ^{13}C NMR (126 mHz, $CDCl_3$, 25°C): δ = 164.88, 133.56, 61.21, 14.02.

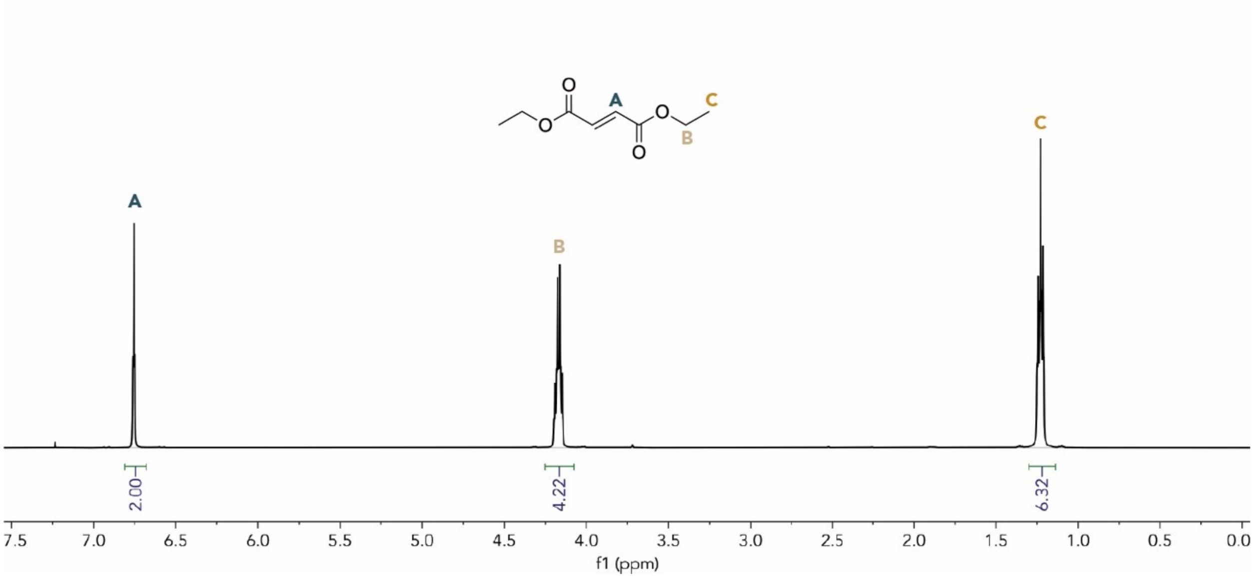

Figure S1-A1: ^{1}H NMR spectra of diethyl fumarate in $CDCl_3$.

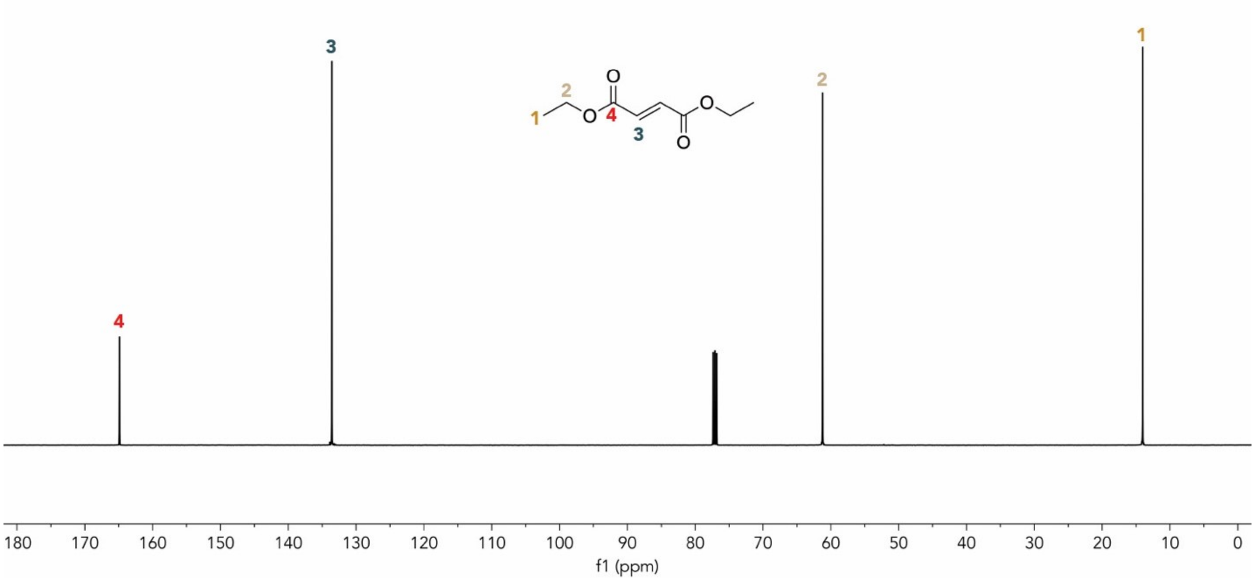

Figure S1-A2: ^{13}C NMR spectra of diethyl fumarate in $CDCl_3$.

Diallyl succinate (DS). ^{1}H NMR (500 mHz, $CDCl_3$, 25°C): δ = 5.85 (ddt, J = 16.5, 11.0, 5.7 Hz, 2H), 5.32 – 5.12 (m, 4H), 4.54 (dt, J = 5.8, 1.6, 4H), 2.61 (s, 2H). ^{13}C NMR (126 mHz, $CDCl_3$, 25°C): δ = 171.82, 132.02, 118.18, 65.30, 28.98.

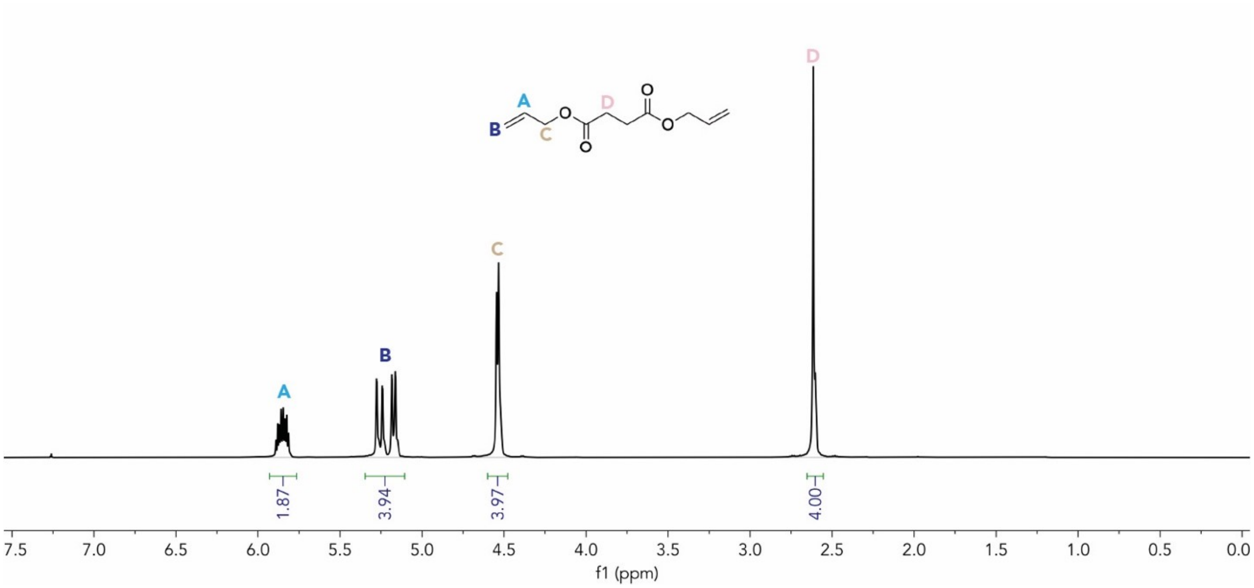

Figure S1-B1: ^{1}H NMR spectra of diallyl succinate in $CDCl_3$.

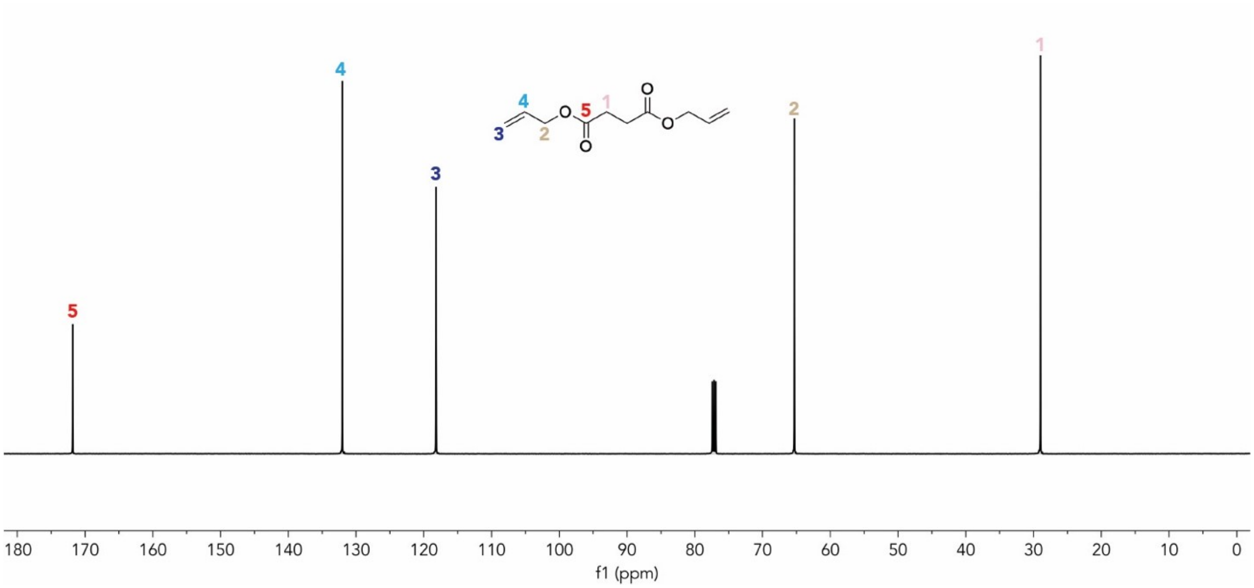

Figure S1-B2: ^{13}C NMR spectra of diallyl succinate in $CDCl_3$.

Diallyl trans-3-hexendioate (DT3HD). ^{1}H NMR (500 mHz, $CDCl_3$, 25°C): 5.90 (ddt, *J* = 16.4, 10.8, 5.7 Hz, 1H), 5.71 (tt, *J* = 3.8, 1.8 Hz, 1H), 5.31 (dt, *J* = 17.1, 1.9 Hz, 1H), 5.23 (d, *J* = 10.5 Hz, 1H), 4.58 (d, *J* = 5.7 Hz, 2H), 3.18 – 3.09 (m, 2H). ^{13}C NMR (126 mHz, $CDCl_3$, 25°C): δ = 171.08, 132.02, 125.92, 118.32, 65.31, 37.75

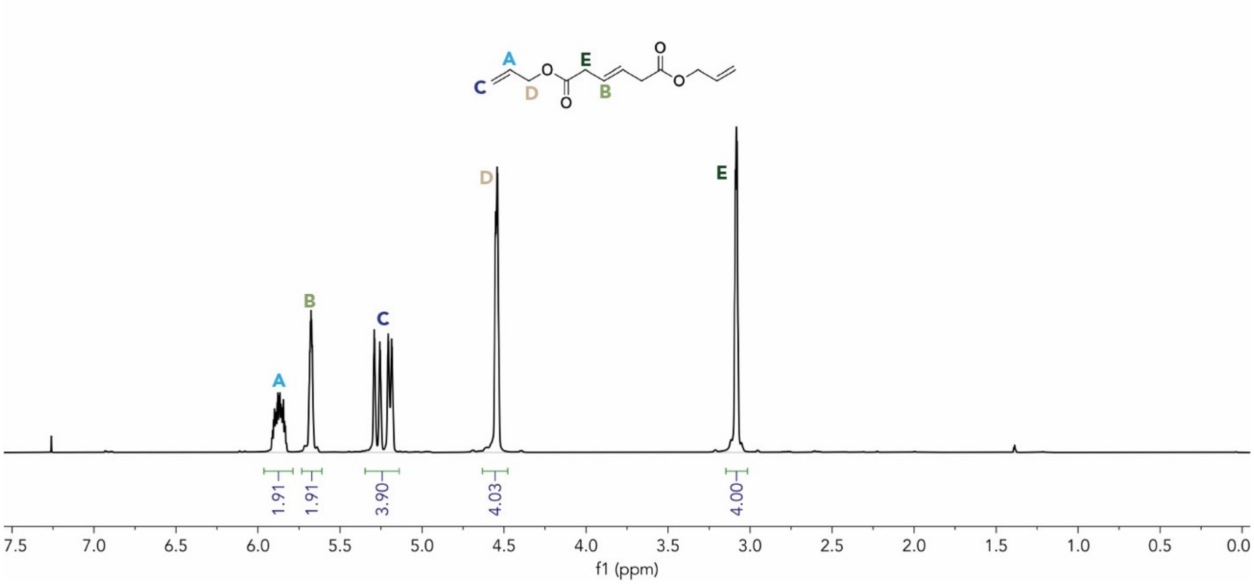

Figure S1-C1: ^{1}H NMR spectra of diallyl trans-3-hexendioate in $CDCl_3$.

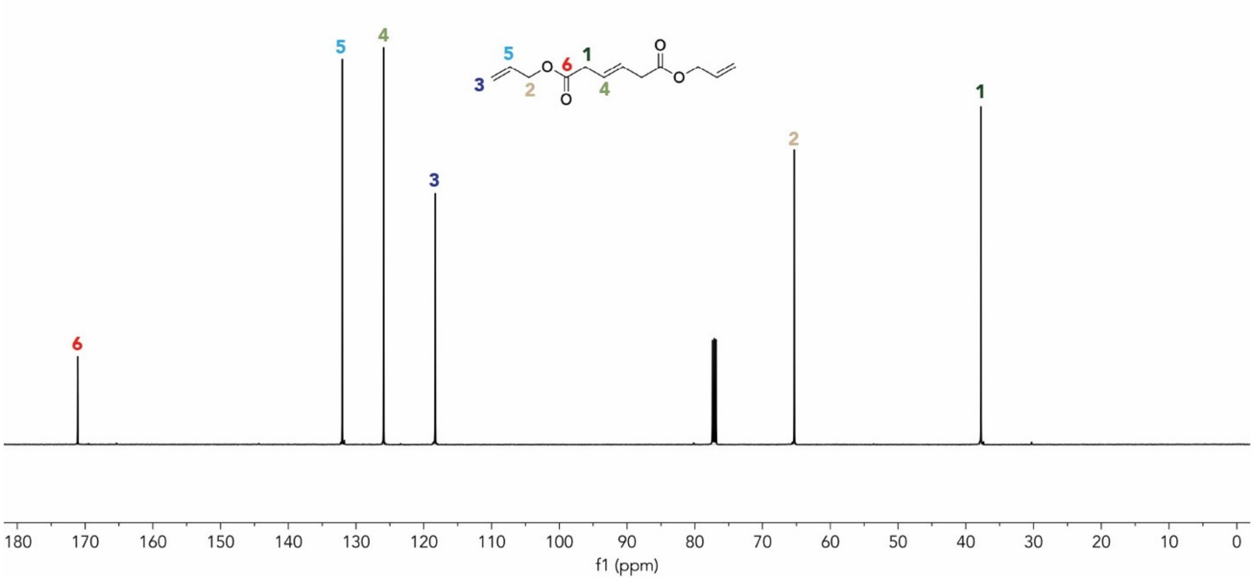

Figure S1-C2: ^{13}C NMR spectra of diallyl trans-3-hexendioate in $CDCl_3$.

Diallyl fumarate (DF). ^{1}H NMR (500 mHz, $CDCl_3$, 25°C): δ = 6.88 – 6.82 (m, 1H), 6.84 (s, 1H), 5.96 – 5.83 (m, 2H), 5.31 (ddq, *J* = 17.2, 4.9, 1.6 Hz, 2H), 5.26 – 5.19 (m, 2H), 4.65 (tq, *J* = 5.0, 1.7 Hz, 4H); ^{13}C NMR (126 mHz, $CDCl_3$, 25°C): δ = 164.42, 133.59, 131.49, 118.78, 65.82.

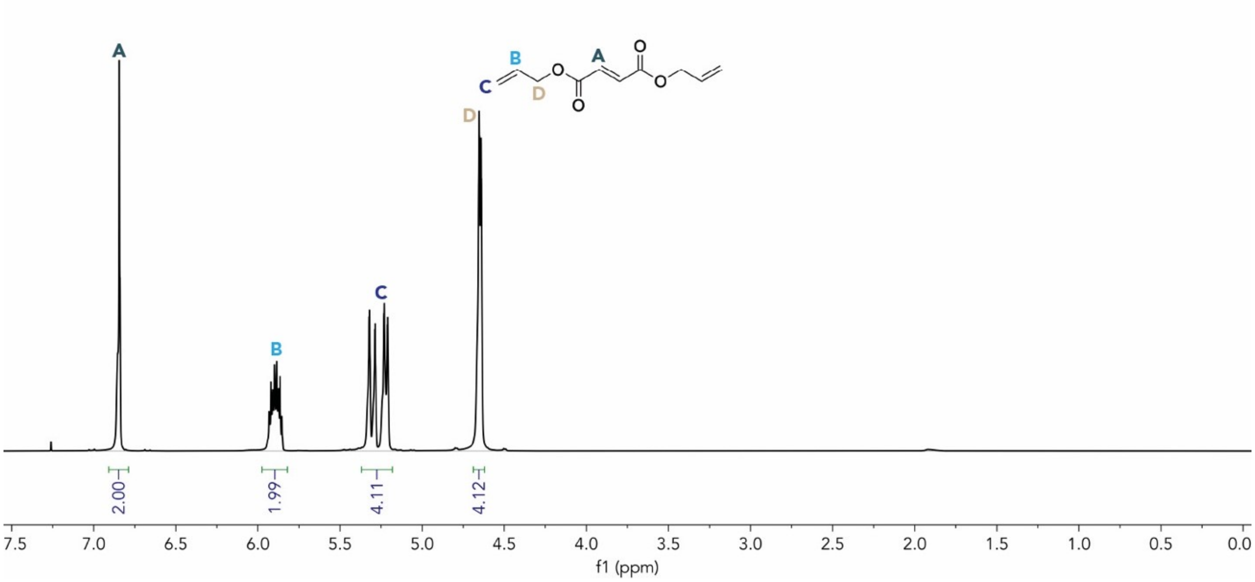

Figure S1-D1: ^{1}H NMR spectra of diallyl fumarate in $CDCl_3$.

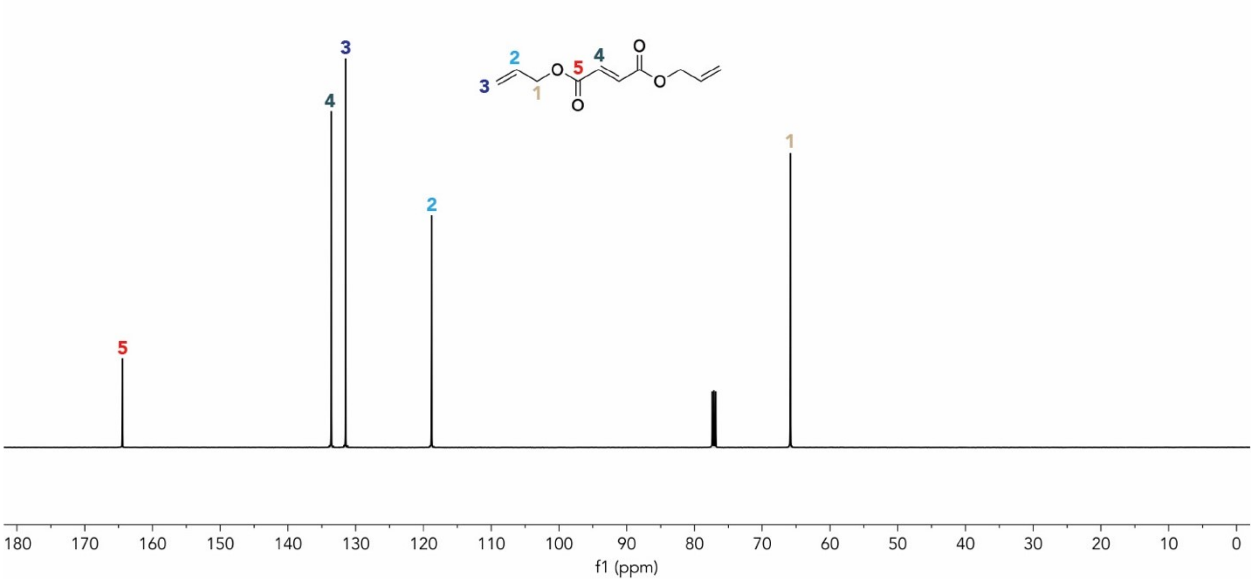

Figure S1-D2: ^{13}C NMR spectra of diallyl fumarate in $CDCl_3$.

2. Small Molecule Reactivity

Mono-thiol Structures

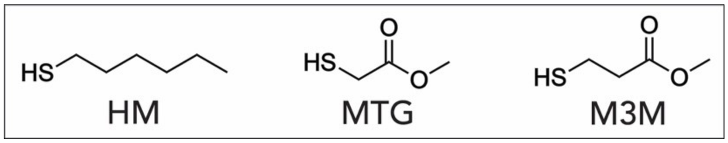

Figure S2-00: Structures of monothiols used in small molecule reactivity studies.

1:1 Ratios

Overview.

To elucidate the relative rates between thiol-ene addition and chain-growth homopolymerization, photoreactions (405 nm, 5mW cm^{-2}) between ene small molecules and monothiols were conducted in a 1:1 allyl:thiol ratio or 1:1 fumarate/maleate:thiol ratio for molecules without allyl groups (DEF, DEM). DS, DEF and DEM benchmarked the addition of thiols to allyl groups, fumarate groups, and maleate groups, respectively, as thiol-ene addition is known to react faster than chain growth of internal enes and allyl ether groups. DF and DM exhibited high conversion of allyl functionalities on similar timescales to DS, implying a similar thiol addition. However, high conversion of internal ene functionality was also observed implying chain growth as overall ene conversion was higher than amount of thiol reactant, which is further corroborated by SEC traces. DT3HD showed the importance of the proximity of carbonyl groups for homopolymerization as the carbon spacing to the double bond disallowed homopolymerization. In addition, the total conversion of internal ene and allyl groups aligns with quantitative consumption of thiol. DM and DEM undergo an isomerization polymerization mechanism as specified in the main text. Of note, formation of *cis* diallyl 3-hexendioate was observed, which is counter to earlier studies of *trans* isomers not converting to the *cis* configuration.[2,3] Among thiols, the conversion of all ene functionalities follows the trend: M3M > HT > MTG.

Conversion of DT3HD with monothiol showed the importance of the proximity of carbonyl groups to the internal ene group. While conversion of the internal group was observed, the total conversion of all ene groups aligned with complete conversion of thiol groups, implying the addition of thiols to the internal ene group. In this system, the carbonyl groups do not provide the same electron withdrawing effect or steric effects on the internal ene, reducing the propensity of homopolymerization and allowing for more thiol addition. This is further corroborated by GPC where no large molecular weight species were observed.

Ene Functionality Conversion Plots.

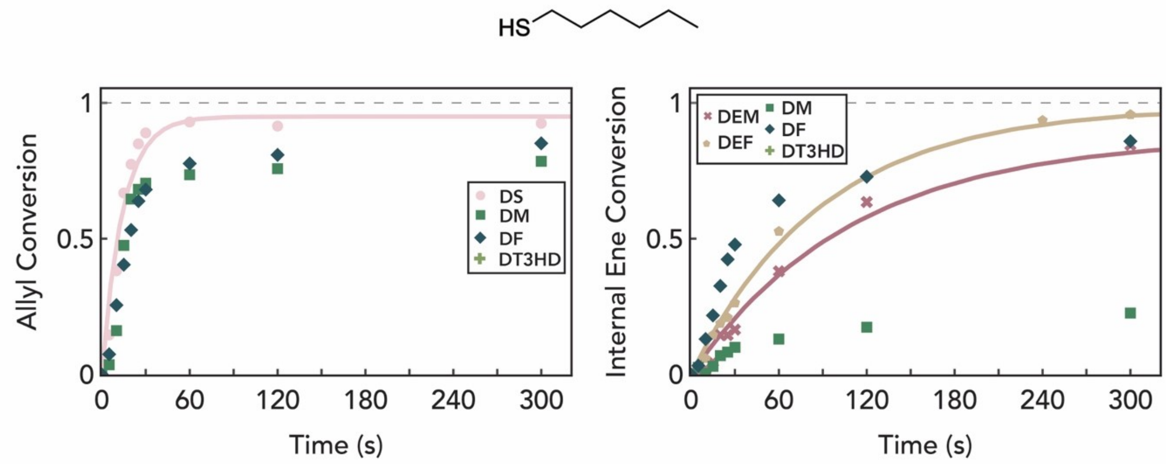

Figure S2-A1: Allyl (left) and internal ene (right) conversion in photoreactions of ene small molecules with n-hexanethiol. Conversions of ene molecules DEF, DEM, and DS are benchmarks for addition of thiol to each ene functionality and are fit to first–order kinetics.

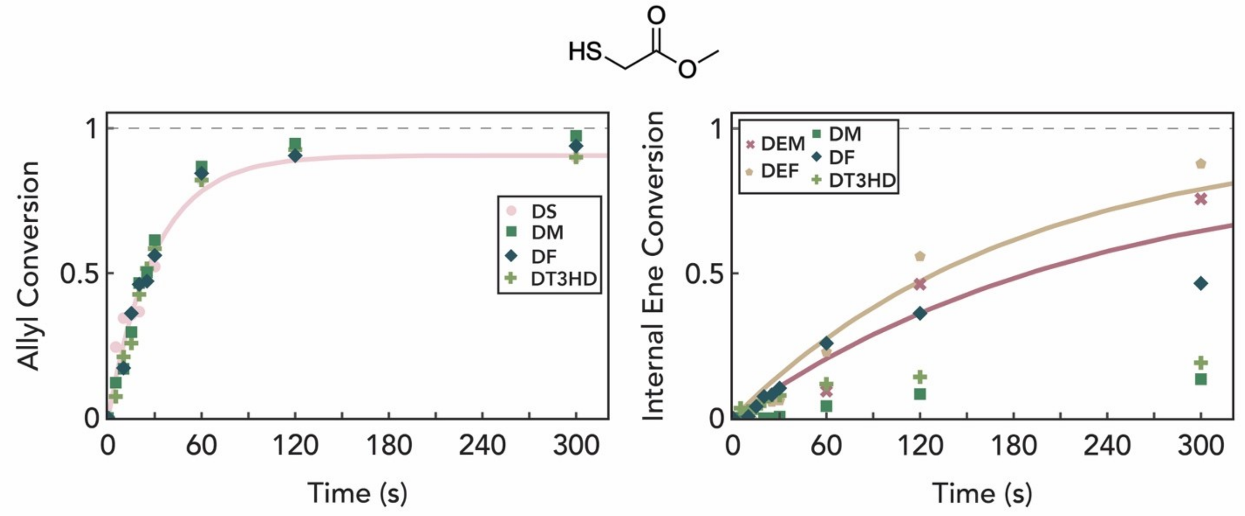

Figure S2-A2: Allyl (left) and internal ene (right) conversion in photoreactions of ene small molecules with methyl thioglycolate. Conversions of ene molecules DEF, DEM, and DS are benchmarks for addition of thiol to each ene functionality and are fit to first–order kinetics.

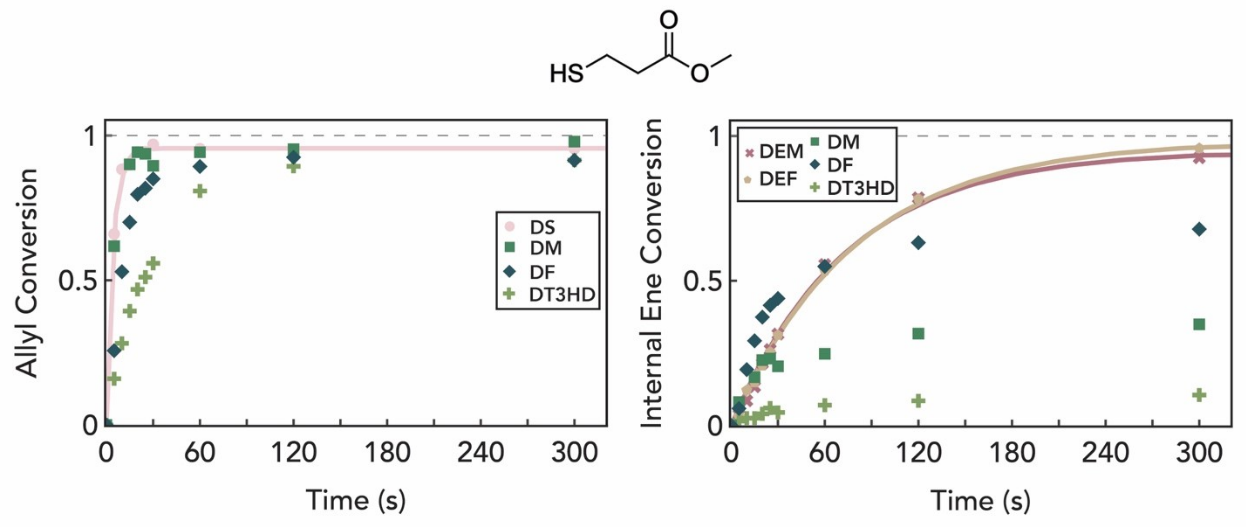

Figure S2-A3: Allyl (left) and internal ene (right) conversion in photoreactions of ene small molecules with methyl 3-mercaptopropionate. Conversions of ene molecules DEF, DEM, and DS are benchmarks for addition of thiol to each ene functionality and are fit to first–order kinetics.

SEC.

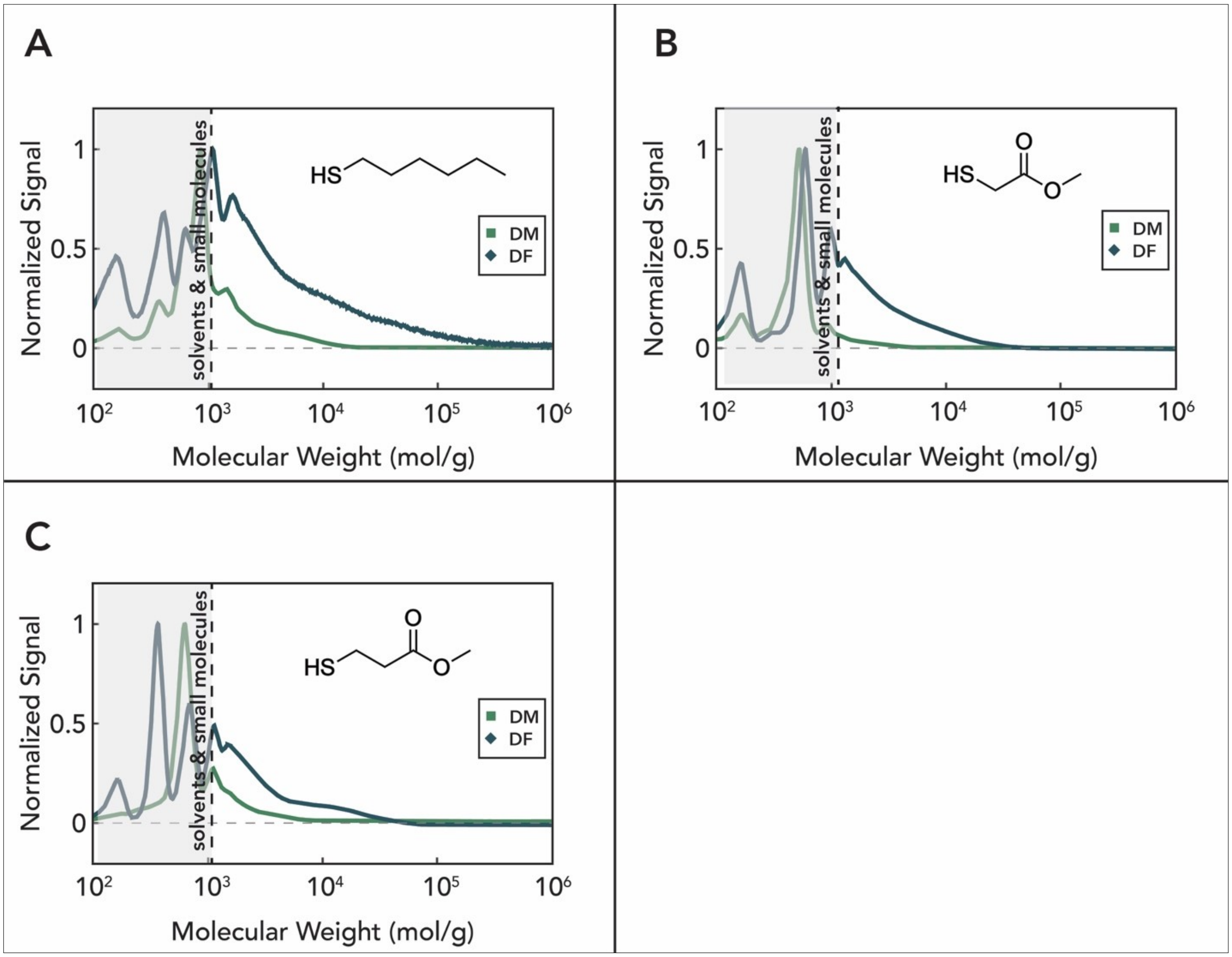

Figure S2-B1: Size exclusion chromatography traces depicting large molecular weight adducts for DM and DF due to chain growth of internal ene group.

SEC Calibration Curve & Retention Time Curves.

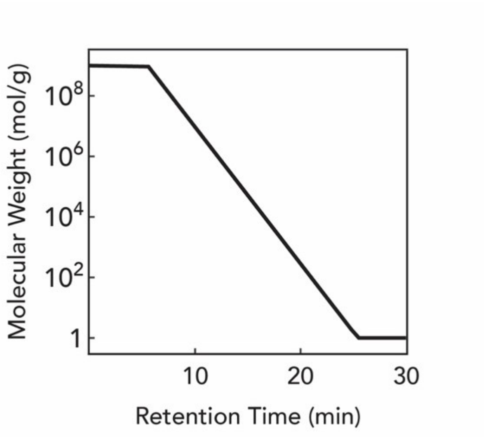

Figure S2-C1: SEC Calibration curve of retention time to molecular weight as measured by polystyrene standards.

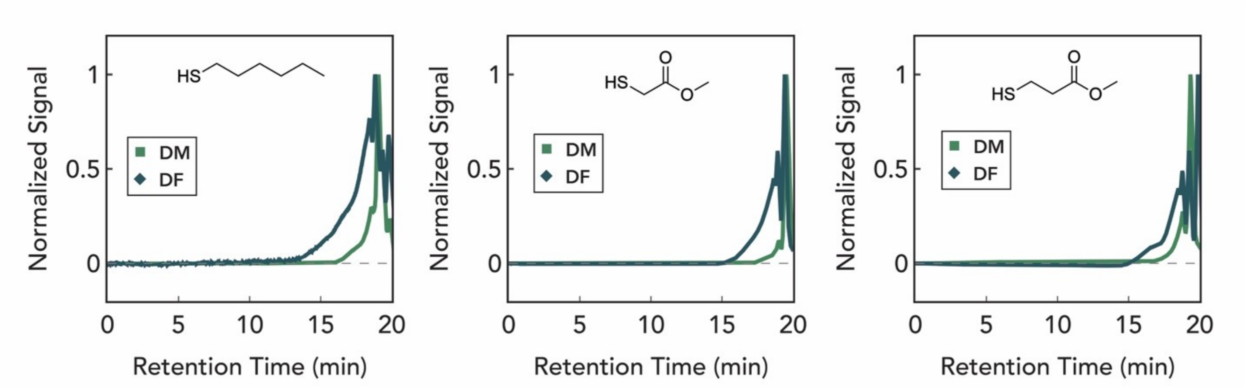

Figure S2-C2: SEC traces against retention time in minutes of 1:1 allyl:thiol photoreactions with HM, MTG, and M3M after 30 minutes.

Stacked Raw NMR Spectra

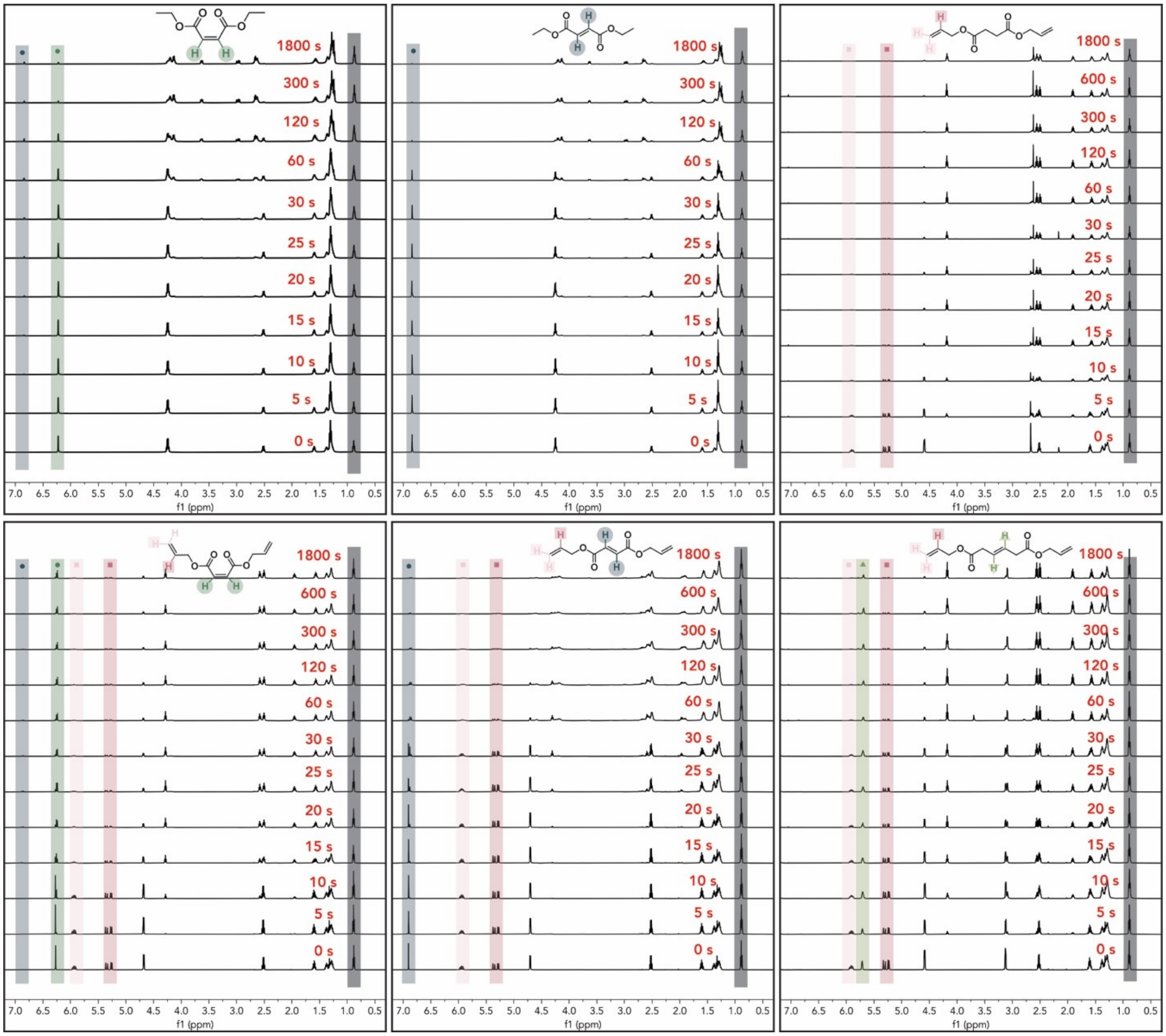

Figure S2-D1: Stacked RAW NMR spectra of photoreactions with hexyl mercaptan in 1:1. The black bar indicated the stagnant -CH_3 peak of the thiol used to normalize.

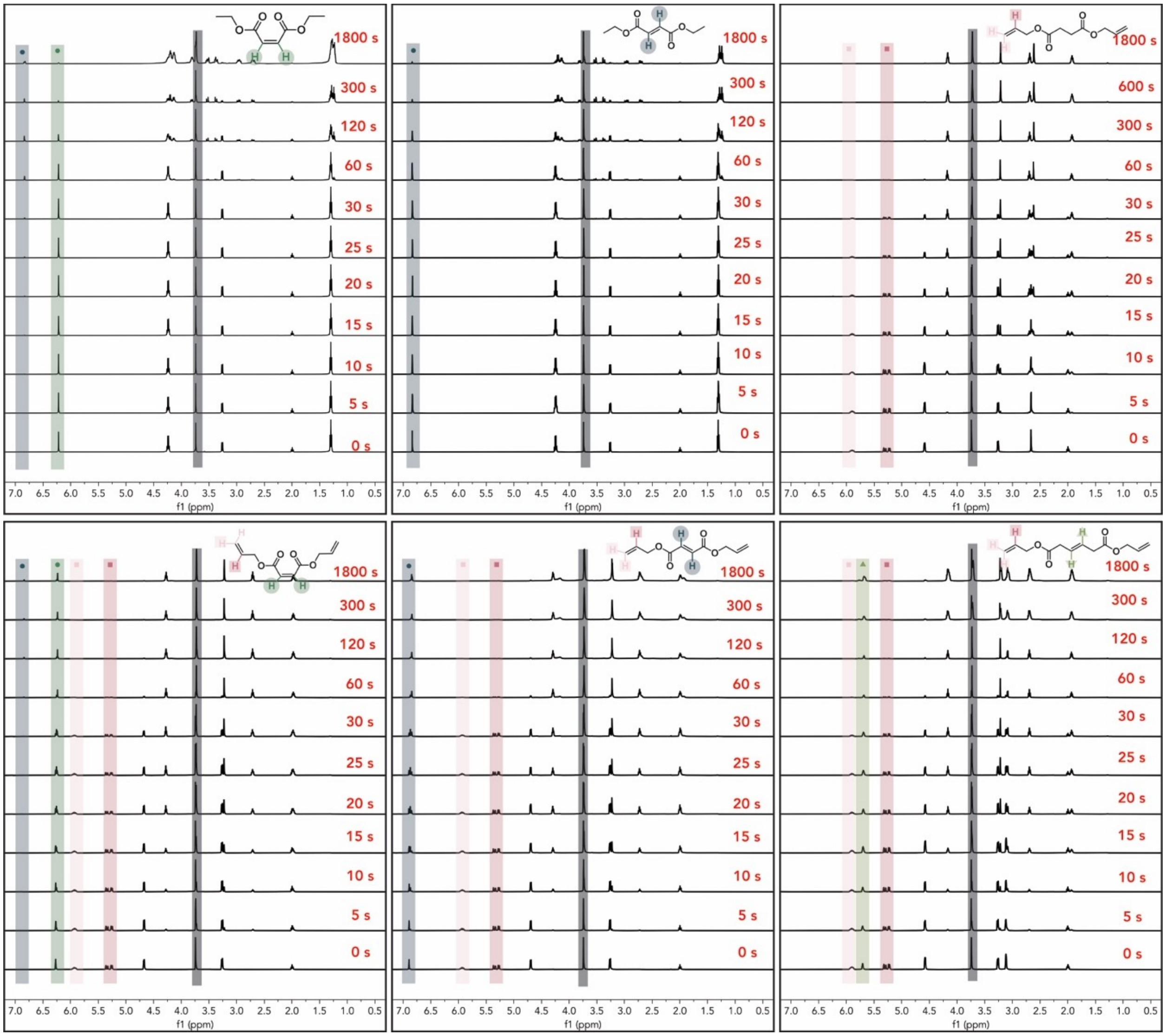

Figure S2-D2: Stacked RAW NMR spectra of photoreactions with methyl thioglycolate in 1:1. The black bar indicated the stagnant -CH_3 peak of the thiol used to normalize.

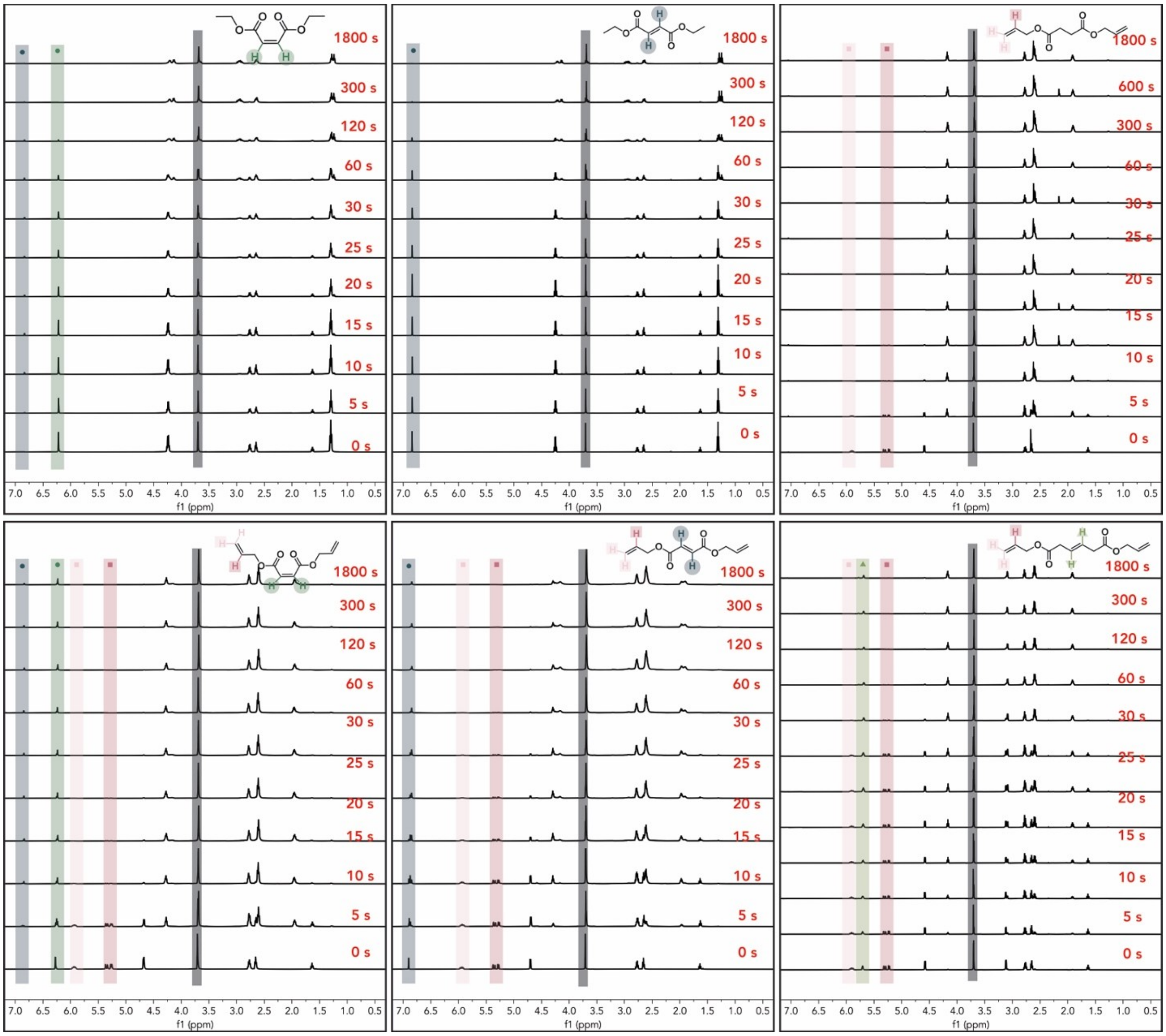

Figure S2-D3: Stacked RAW NMR spectra of photoreactions with methyl 3-mercaptopropionate in 1:1. The black bar indicated the stagnant -CH_3 peak of the thiol used to normalize.

2:1 Ratios

Overview.

To further study the extent of chain-growth homopolymerization between ene groups, reactions between ene small molecules and monothiols were conducted in a 2:1 allyl:thiol ratio or 2:1 fumarate/maleate:thiol ratio for DEF and DEM. This allowed excess ene groups to be present in the system. As expected, no homopolymerization of DS along with limited half conversion was observed. Interestingly, the same was observed of DEF and DEM, implying the need for allyl groups in this homopolymerization mechanism. DF and DM showed conversion of both ene groups due to the additional chain growth mechanism. DF formed an insoluble network polymer at final illumination timepoints, suggesting some cross-reaction between fumarate and allyl ether groups. The same isomerization mechanism and thiol reactivity was observed.

Conversion.

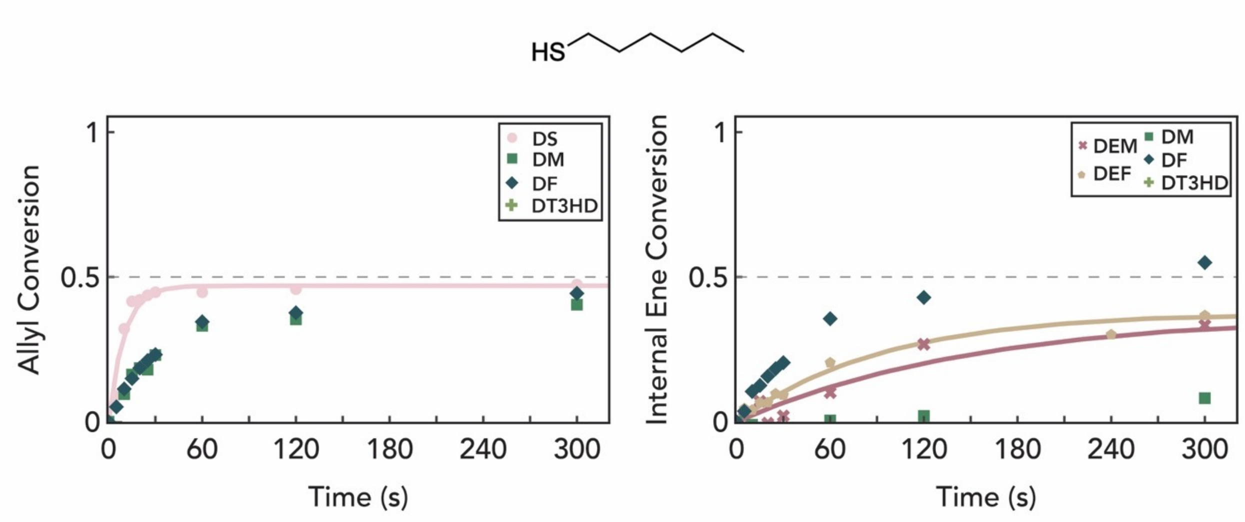

Figure S2-E1: Allyl (left) and internal ene (right) conversion in photoreactions of ene small molecules with n-hexanethiol in 2:1 ratio. Conversions of ene molecules DEF, DEM, and DS are benchmarks for addition of thiol to each ene functionality and are fit to first–order kinetics.

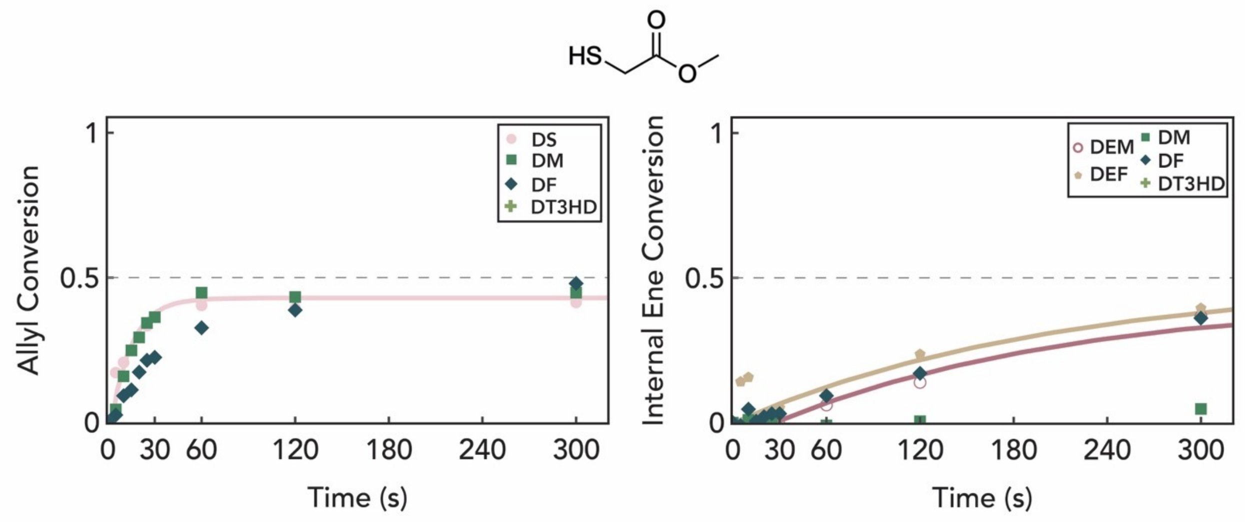

Figure S2-E2: Allyl (left) and internal ene (right) conversion in photoreactions of ene small molecules with methyl thioglycolate in 2:1 ratio. Conversions of ene molecules DEF, DEM, and DS are benchmarks for addition of thiol to each ene functionality and fit to first–order kinetics.

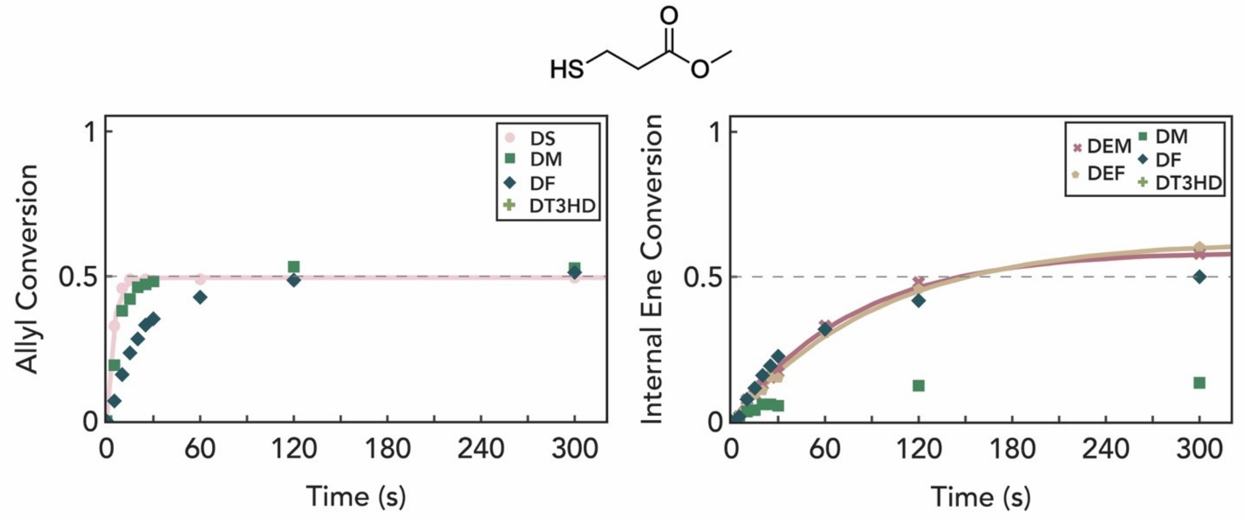

Figure S2-E3: Allyl (left) and internal ene (right) conversion in photoreactions of ene small molecules with methyl 3-mercaptopropionate in 2:1 ratio. Conversions of ene molecules DEF, DEM, and DS are benchmarks for addition of thiol to each ene functionality and fit to first–order kinetics.

Stacked Raw NMR Spectra.

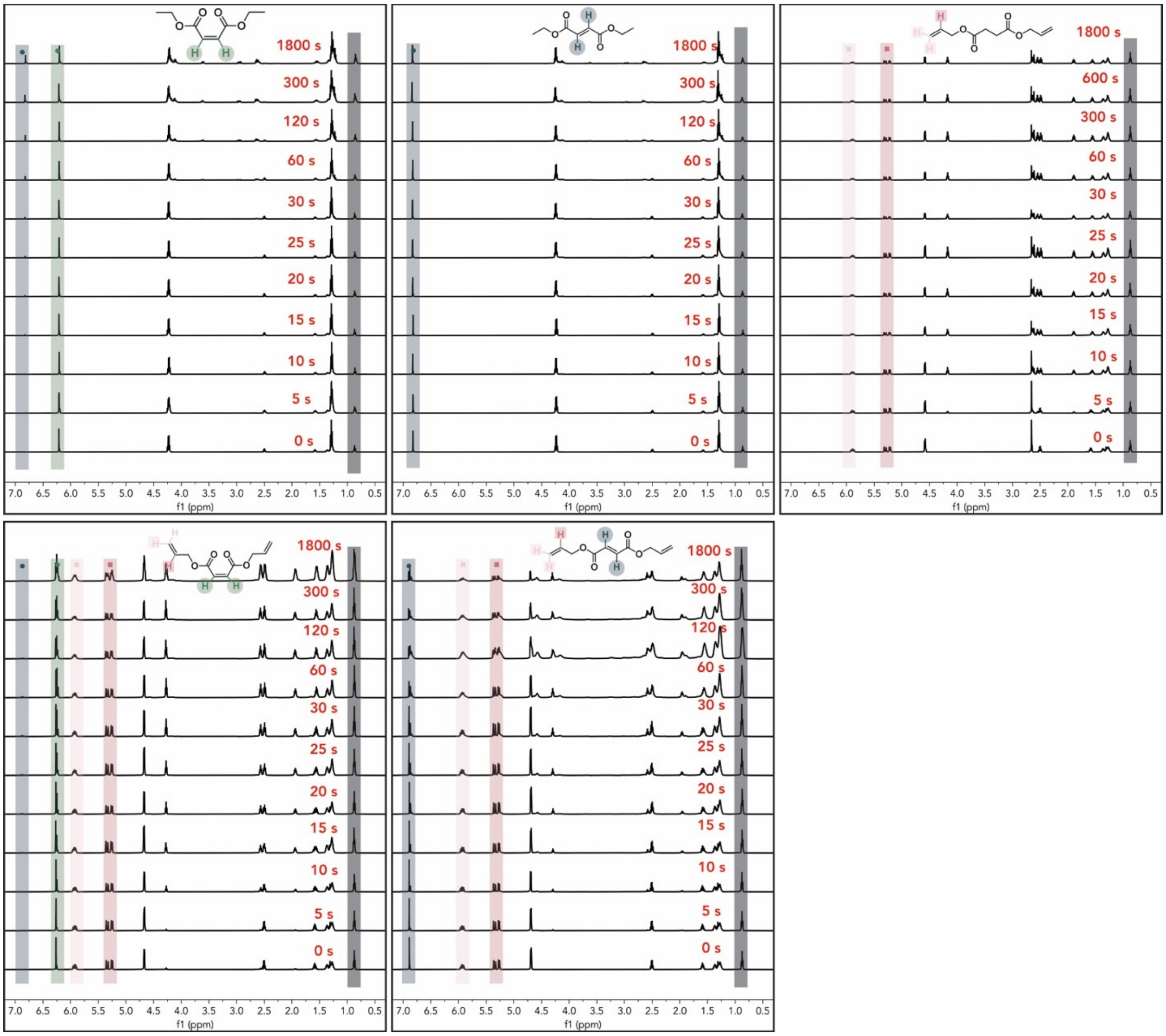

Figure S2-F1: Stacked RAW NMR spectra of photoreactions with hexyl mercaptan in 2:1.

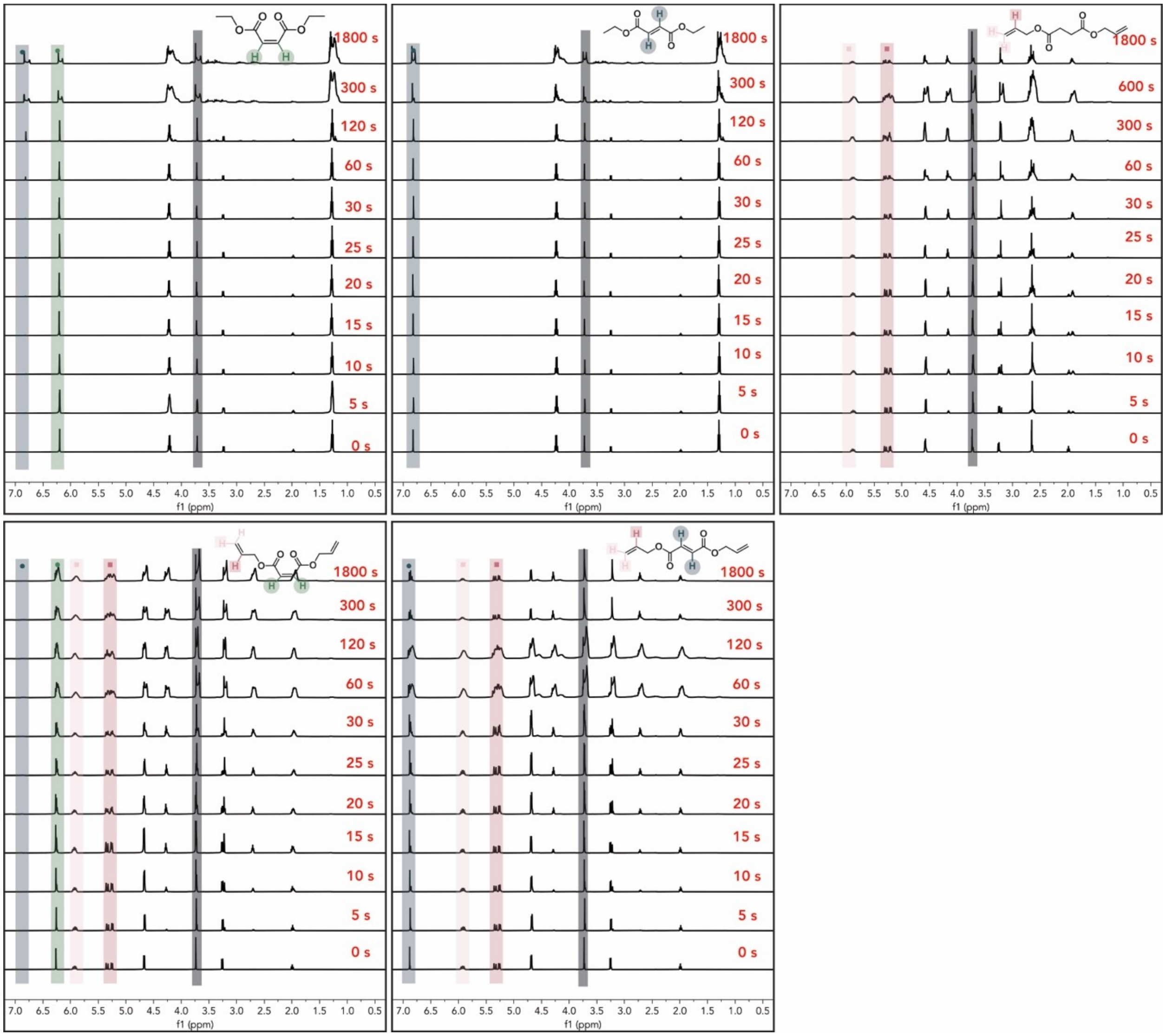

Figure S2-F2: Stacked RAW NMR spectra of photoreactions with methyl thioglycolate in 2:1.

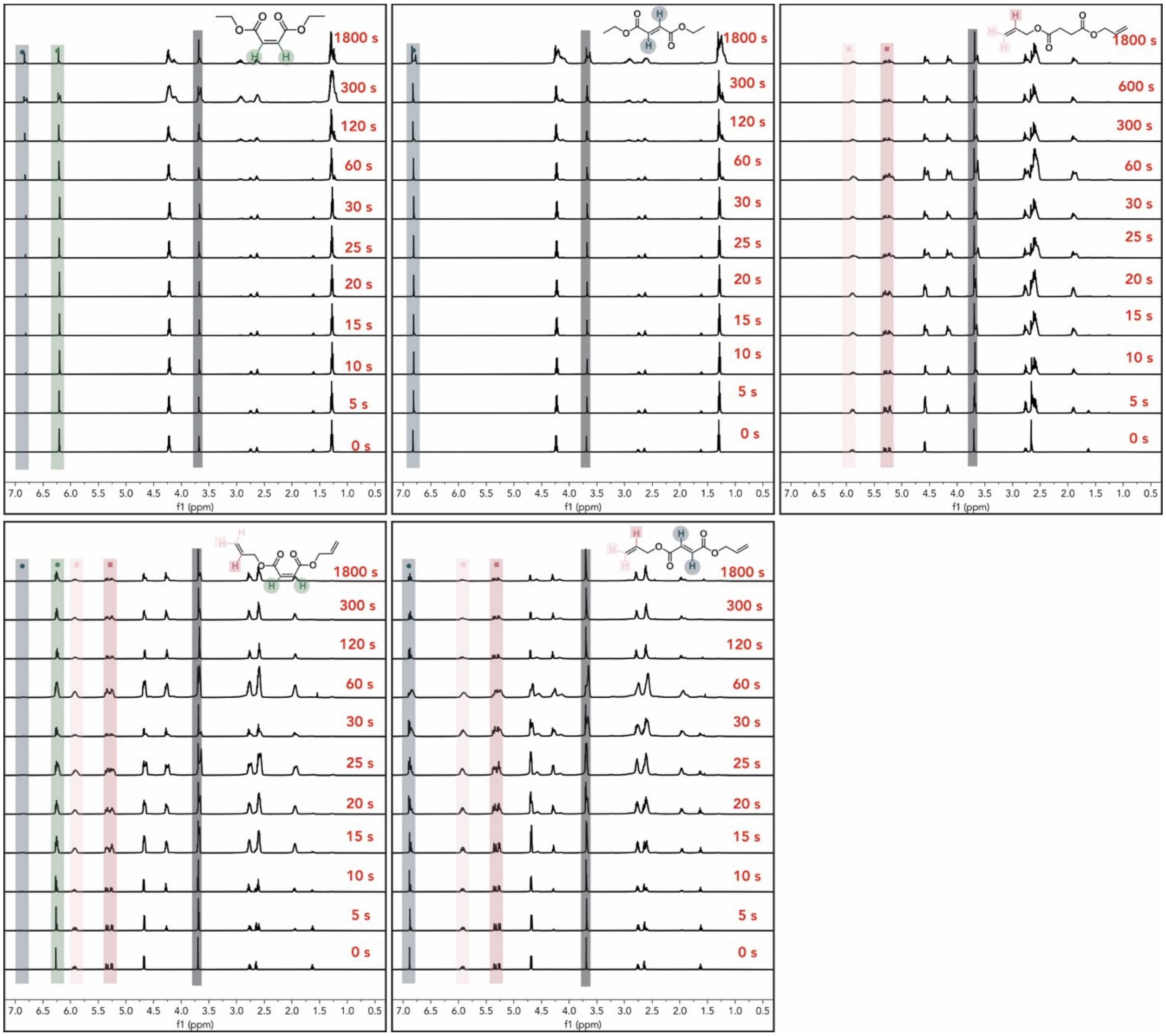

Figure S2-F3: Stacked RAW NMR spectra of photoreactions with methyl 3-mercaptopropionate in 2:1.

R^2 Values for First-Order Kinetic Fitting

Fitting the data to first order–kinetics with the equation:

$$conversion = 1 - \frac{Integration_{t,f.g.}}{Integration_{0,f.g.}} = a(1 - \exp(-k * t))$$

	DS	DM	DF	DT3HD
hexyl mercaptan	0.973	0.918	0.965	0.997
methyl thioglycolate	0.969	0.988	0.972	0.987
methyl 3-mercaptopropionate	0.998	0.994	0.992	0.998

Figure S2–G1: R^2 scoring criteria for first order kinetics onto conversions of thiol and allyl groups for 1:1 ratio.

	DEM	DEF	DM	DF	DT3HD
hexyl mercaptan	0.985	0.997	0.976	0.975	0.926
methyl thioglycolate	0.913	0.953	0.789	0.975	0.969
methyl 3-mercaptopropionate	0.997	0.999	0.924	0.979	0.961

Figure S2–G2: R^2 scoring criteria for first order kinetics onto conversions of thiol and internal ene groups for 1:1 ratio.

Isomerization

Overview

Internal *cis* maleic groups are observed to isomerize into the more energetically favored *trans* fumaric groups as noted in prior literature.[2,3] This is facilitated by the reversibility of thiyl radical addition to internal *cis* unsaturated units which can drive isomerization via rotation about the C-C bond upon thioether formation followed by β-elimination to yield the new stereoisomer. Interestingly, we observe the isomerization of *trans* 3-hexene to *cis* 3-hexene groups.

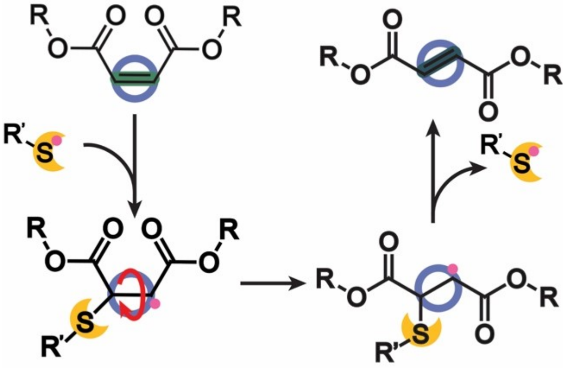

Figure S2–H1: Reversible thiyl addition on to maleic groups facilitates isomerization.

1a1t ratios

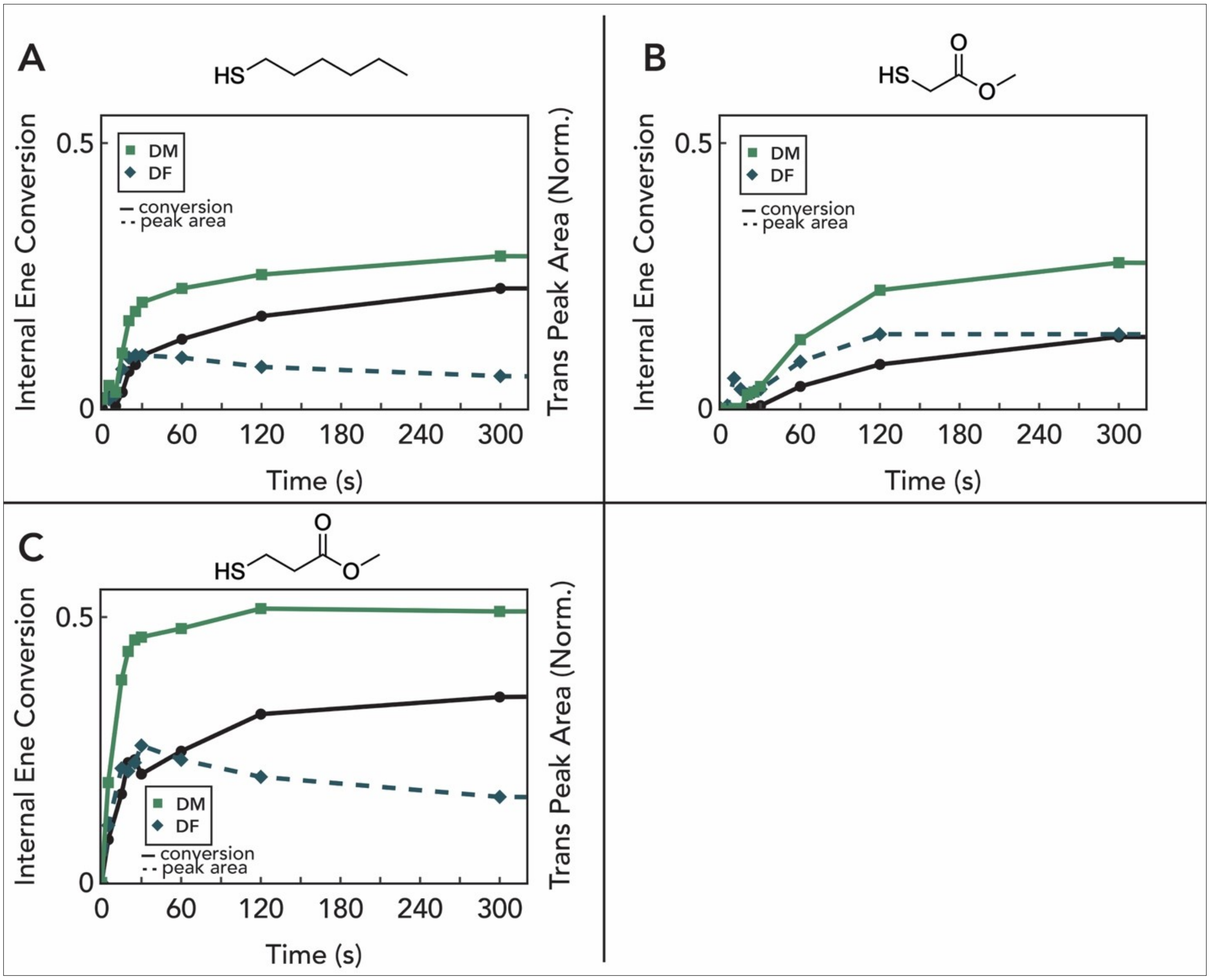

Figure S2-H2: Isomerization from *cis* maleate to *trans* fumarate during photoreaction of diallyl maleate.

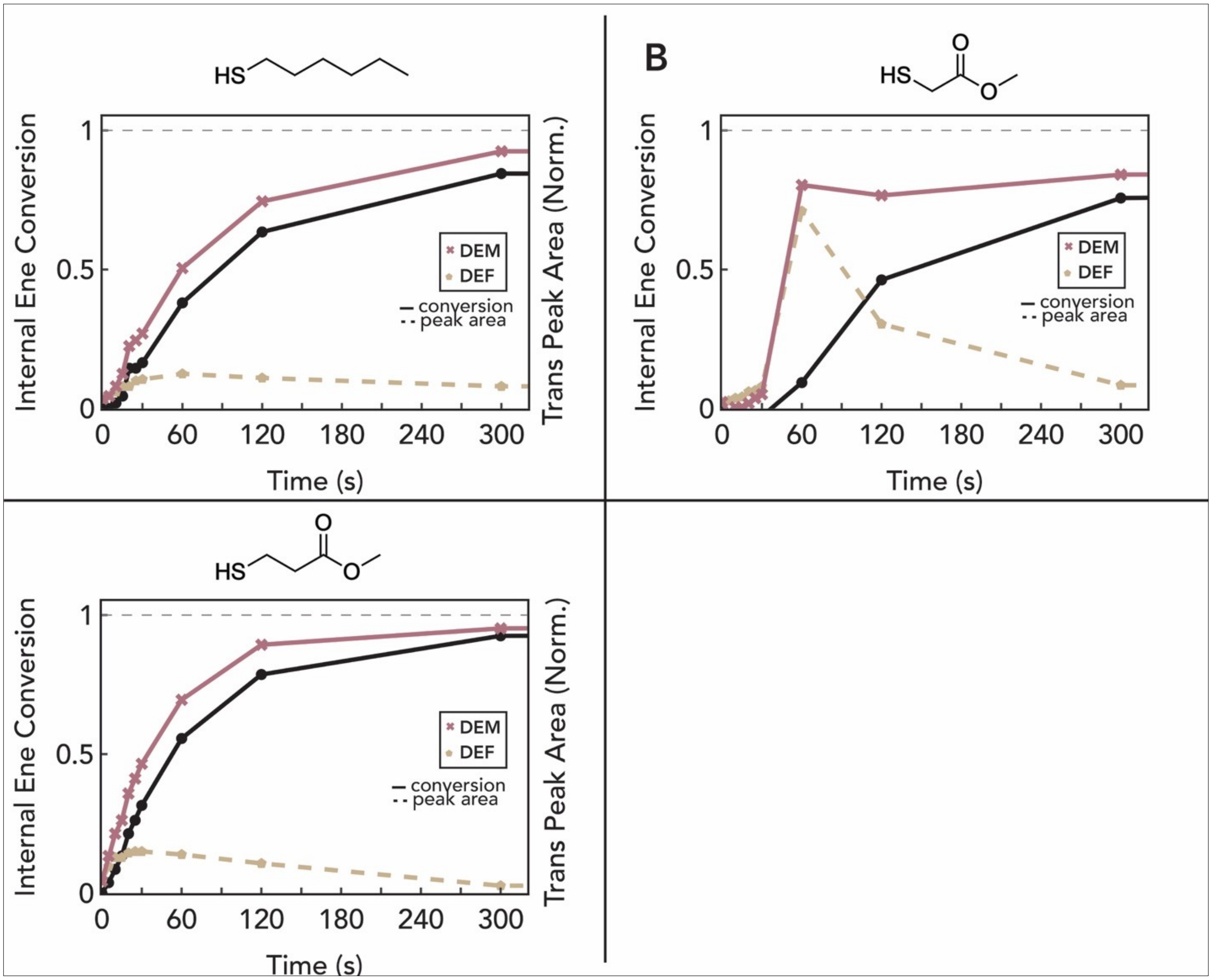

Figure S2-H3: Isomerization from *cis* maleate to *trans* fumarate during photoreaction of diethyl maleate.

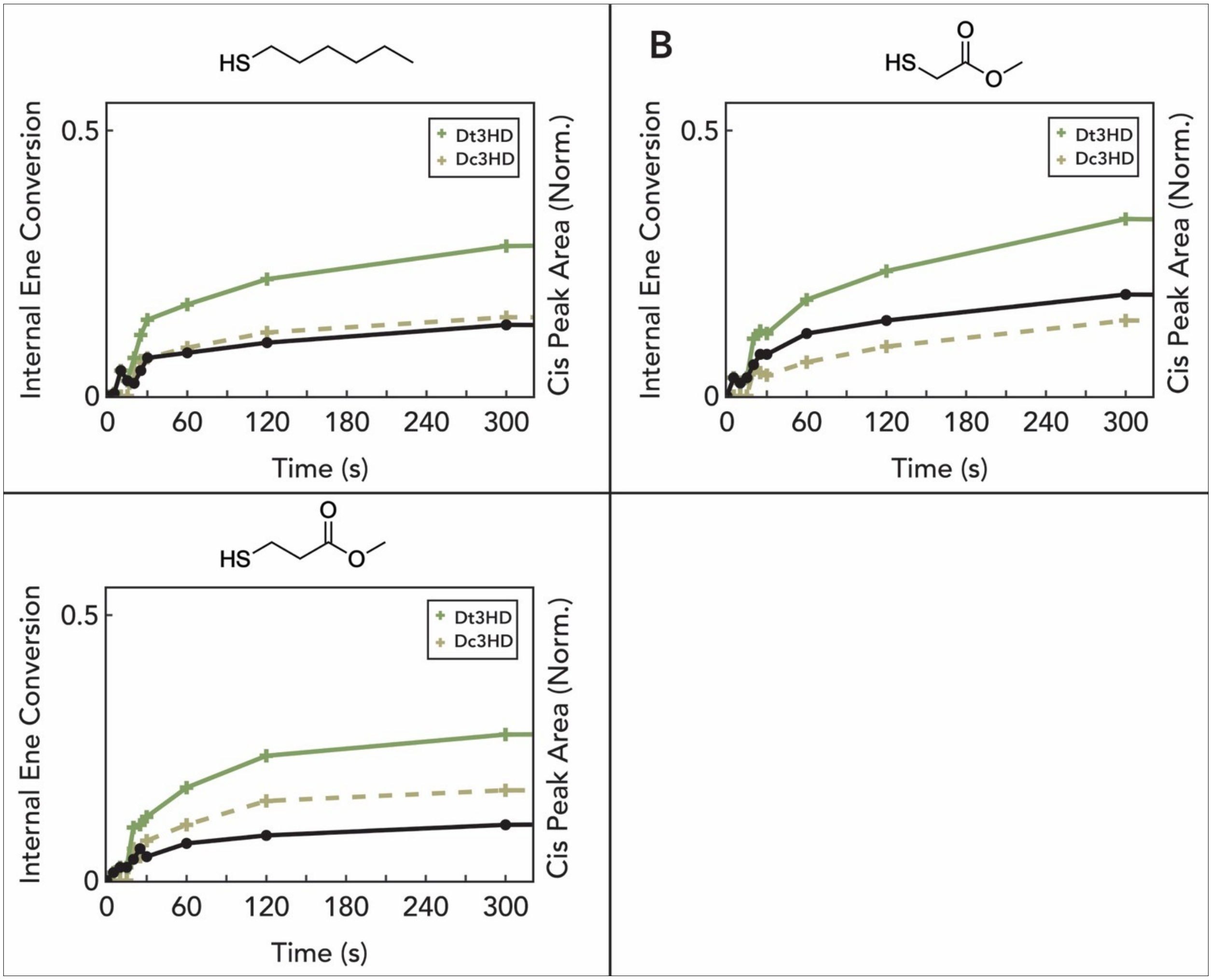

Figure S2-H4: Isomerization from *trans* ene to *cis* ene during photoreaction of diallyl *trans* 3-hexendioate.

2a1t ratios

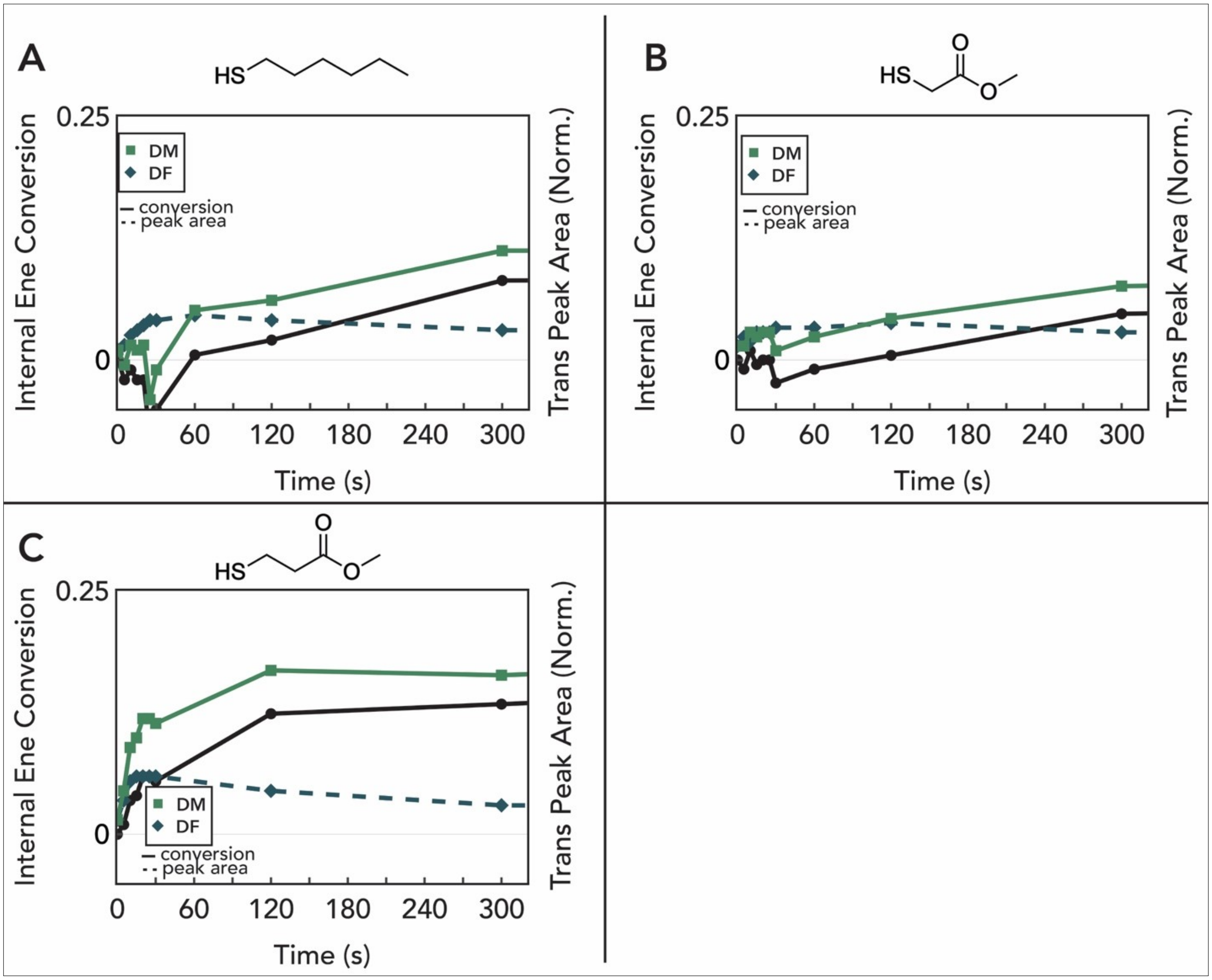

Figure S2-H5: Isomerization from *cis* maleate to *trans* fumarate during photoreaction of diallyl maleate in 2:1.

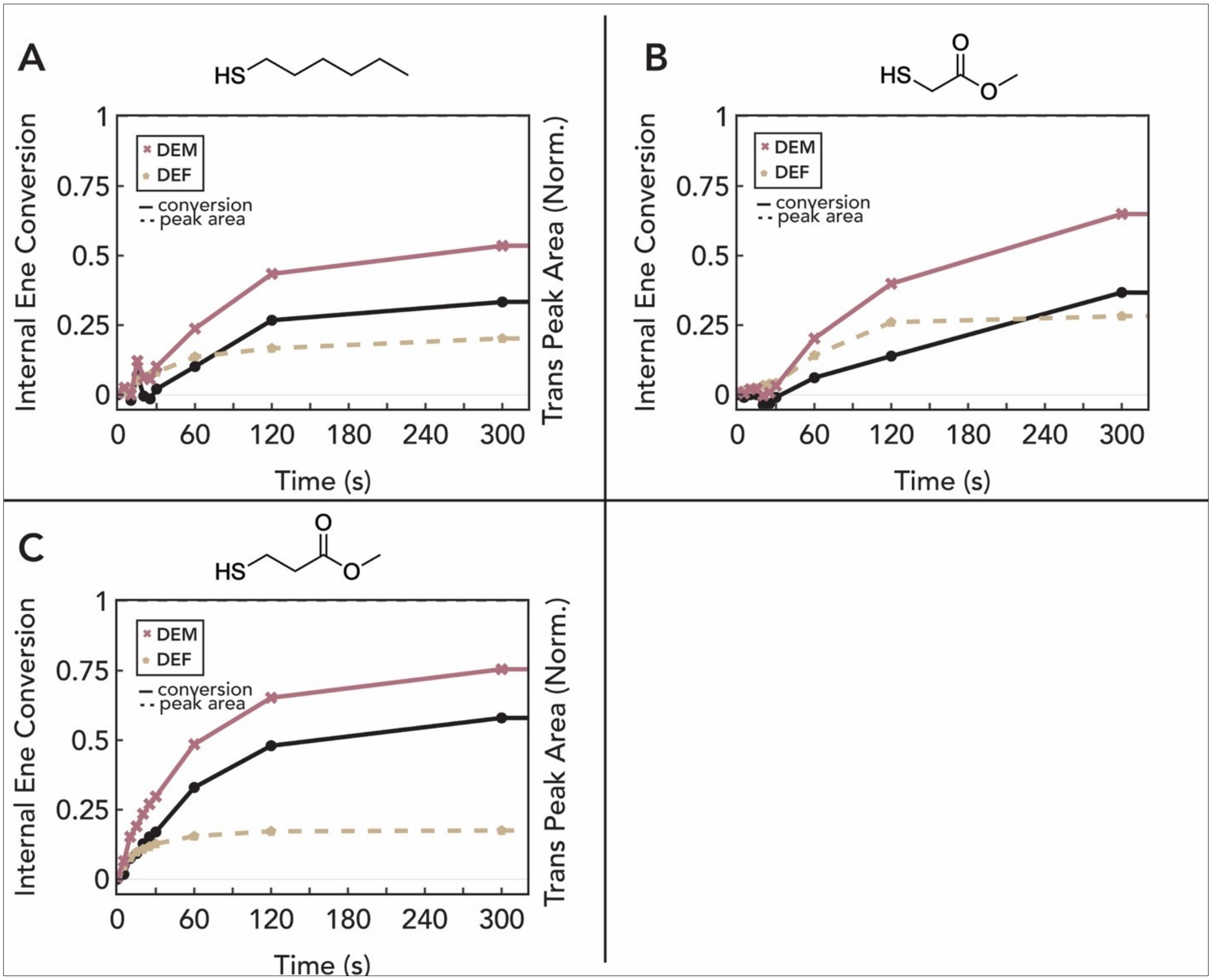

Figure S2-H6: Isomerization from *cis* maleate to *trans* fumarate during photoreaction of diethyl maleate in 2:1.

Real Time FTIR

To reinforce reactivities observed with H^1-NMR, we studied the same photoreactions (405 nm, 5mW cm^{-2}) between ene small molecules and monothiols in specified ratios using RT-FTIR.

1a1t ratios

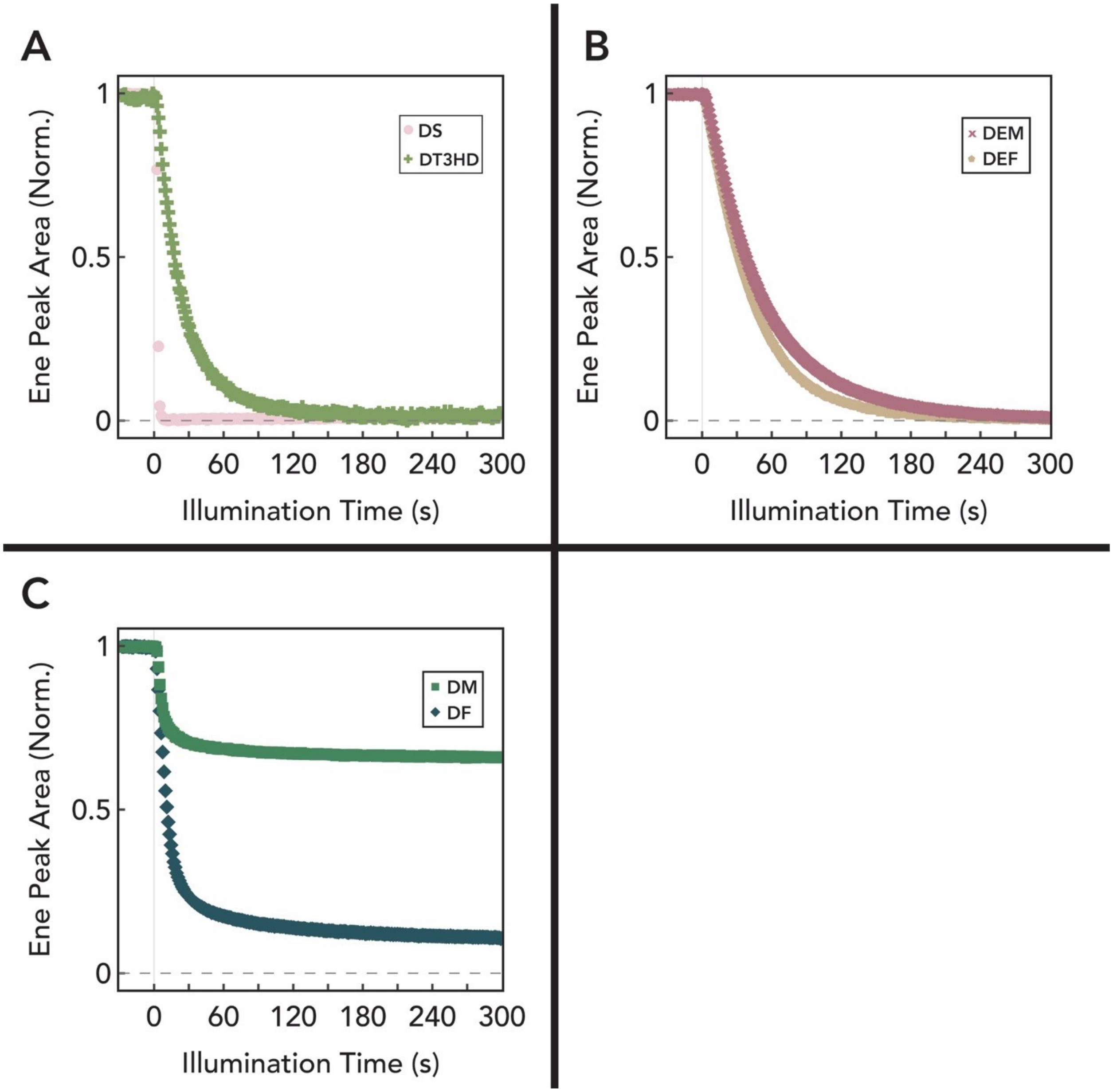

Figure S2-I1: Real-time FTIR monitoring of normalized ene peak area of **1:1** photoreactions between monomers with M3M. This is equivalent to *(A)* conversion of allyl groups for DS and DT3HD monomers, *(B)* conversion of maleate/fumarate groups for DEM/DEF small molecules, but *(C)* definitive conversions of functionalities cannot be stated for DF/DM monomers.

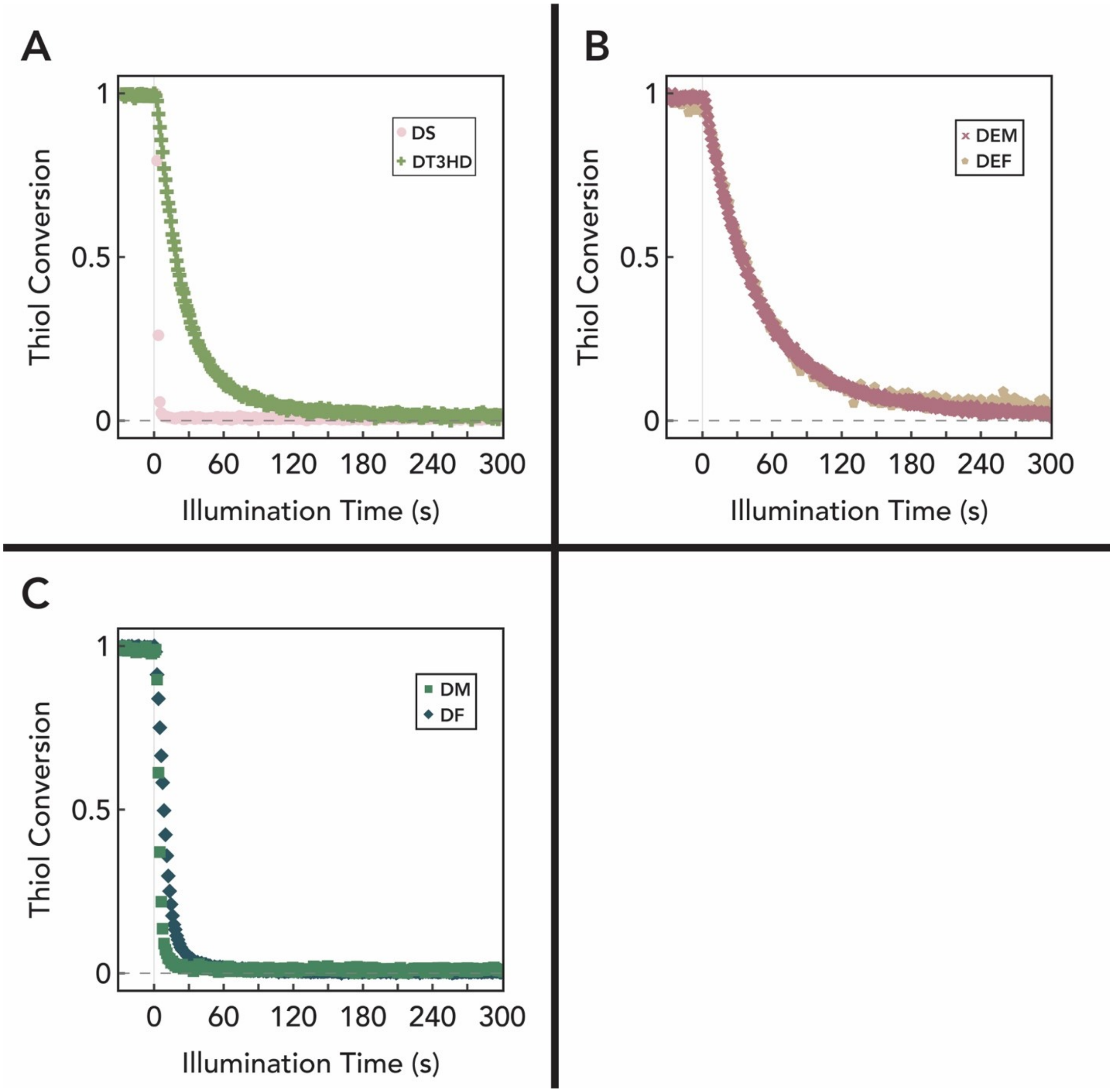

Figure S2-I2: Real-time FTIR monitoring of normalized **thiol** peak area of **1:1** photoreactions between monomers with M3M. This is equivalent to conversion of thiol groups for *(A)* DS and DT3HD monomers, *(B)* DEM/DEF small molecules, and *(C)* DM/DF monomers.

2a1t ratios

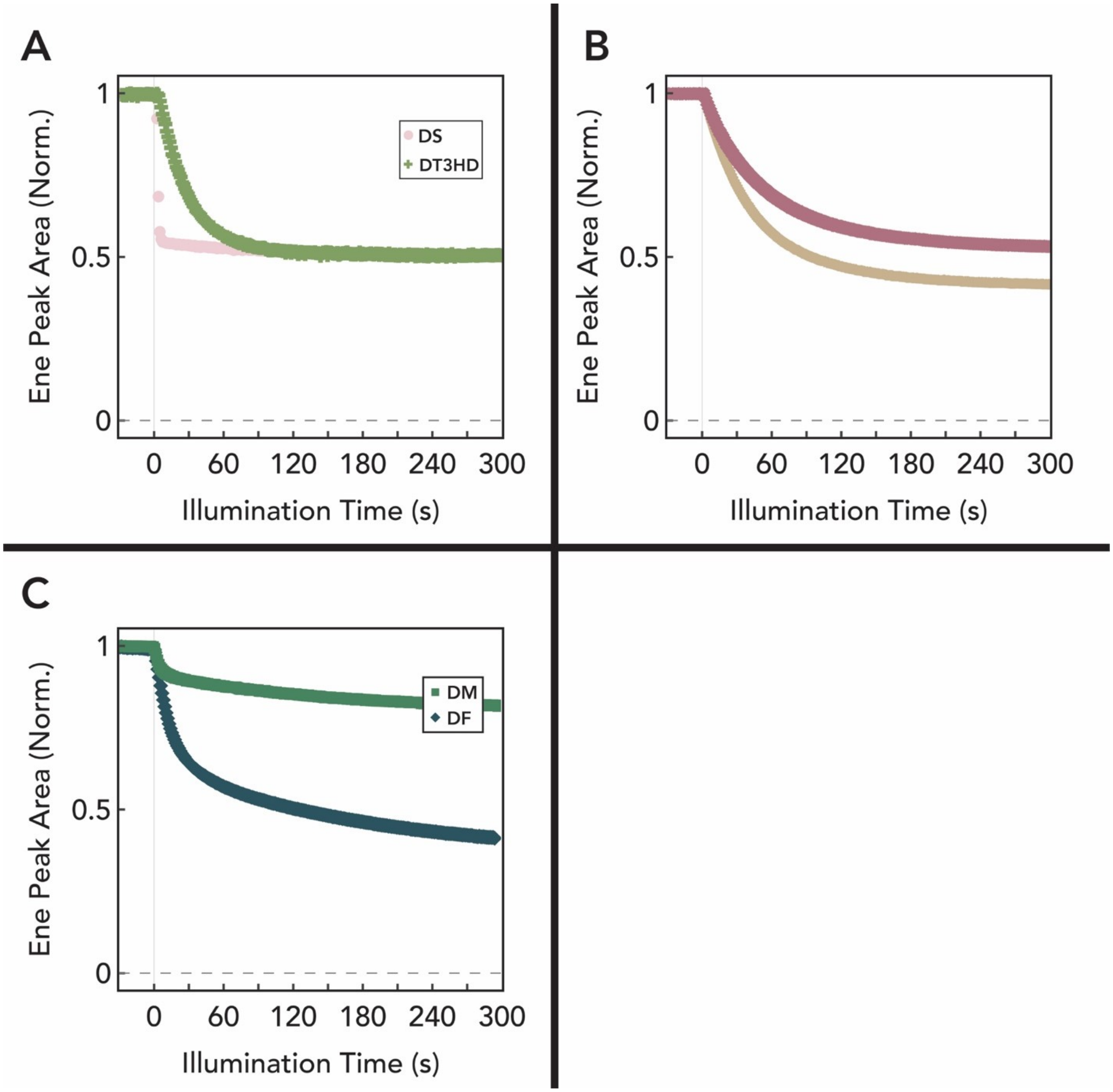

Figure S2-I3: Real-time FTIR monitoring of normalized **ene** peak area of **2:1** photoreactions between monomers with M3M. This is equivalent to *(A)* conversion of allyl groups for DS and DT3HD monomers, *(B)* conversion of maleate/fumarate groups for DEM/DEF small molecules, but *(C)* definitive conversions of functionalities cannot be stated for DF/DM monomers.

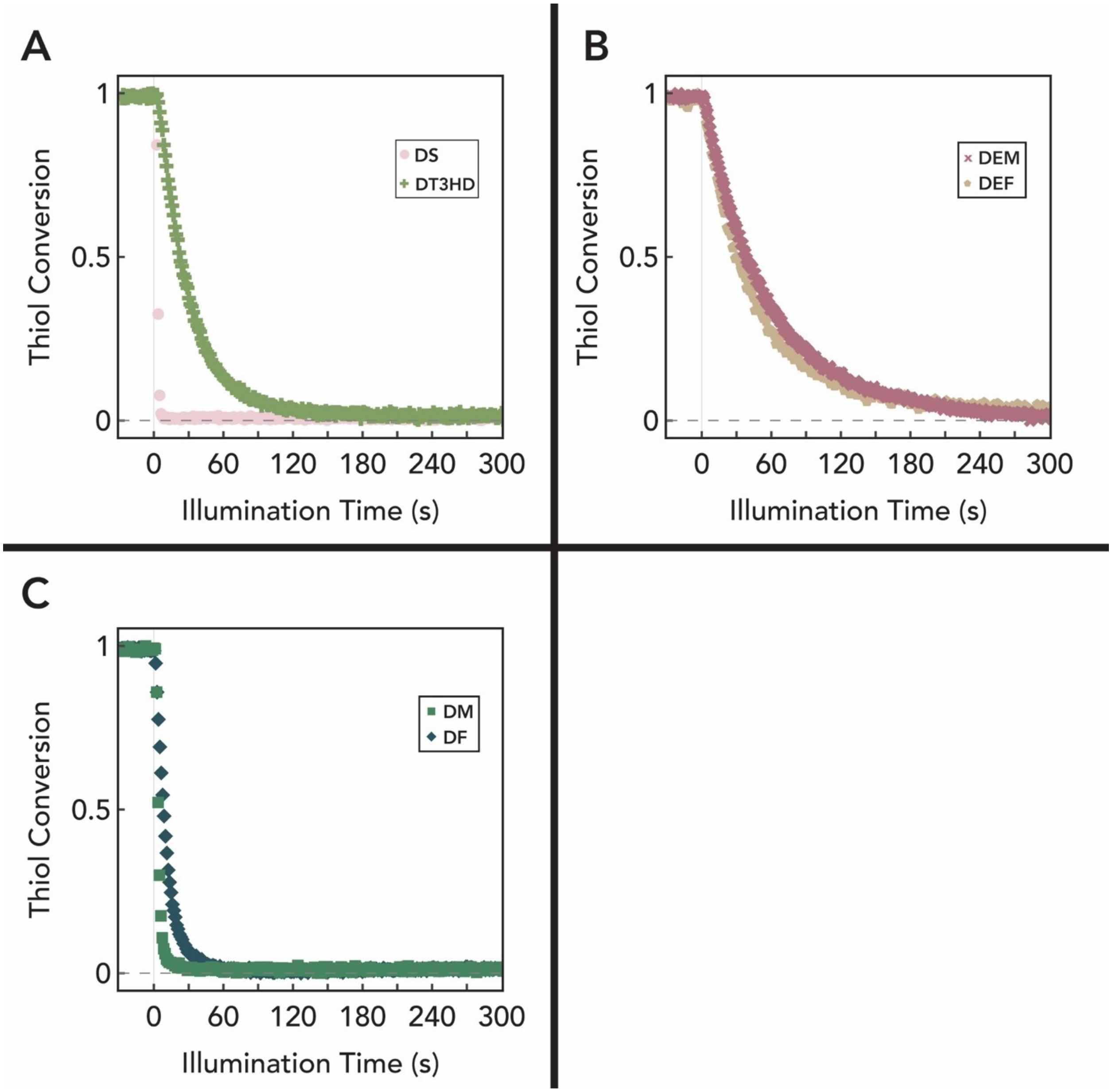

Figure S2-I4: Real-time FTIR monitoring of normalized **thiol** peak area of **2:1** photoreactions between monomers with M3M. This is equivalent to conversion of thiol groups for *(A)* DS and DT3HD monomers, *(B)* DEM/DEF small molecules, and *(C)* DM/DF monomers.

3. Gelation and Thermomechanical Properties

Thiols & Crosslinker:

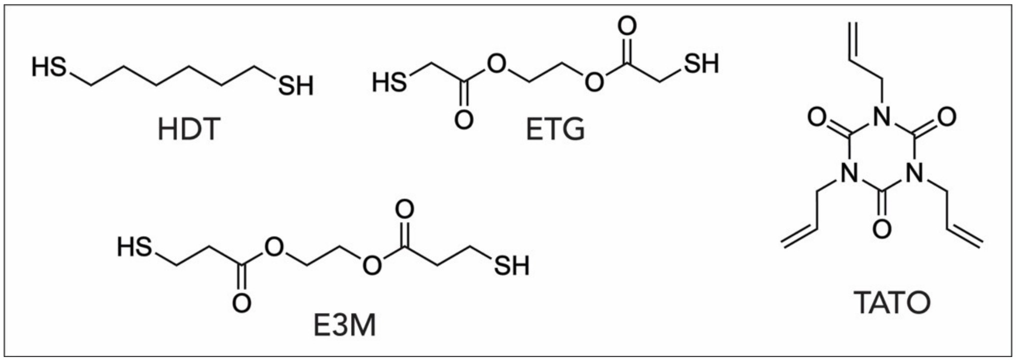

Figure S3-00: Structures of dithiols and crosslinker used in polymer networks.

Network Reactivity and Assembly Studies

Overview

We applied this mixed mechanism reactivity into polymer networks by forming resins with the studied diallyl monomers with 5% TATO (triallyl crosslinker) and dithiol (analogous to the monothiols studied in the NMR studies) in 1:1 allyl:thiol ratio. We measured the consumption of these ene groups under IR and Raman spectroscopy to illustrate the translation of reactivity to network polymers. Due to *trans*-*cis* ester configurations about the internal bond, maleic and fumaric peaks activate under IR despite being centrosymmetric. In addition, since there are more *trans*-*cis* vibrational modes of the maleic peak, it appears at a higher absorbance than the trans fumaric peak. Moreover, these internal ene peaks occur at the same IR stretch as the terminal allyl peaks. Thus, normalized peak area change cannot fully encapsulate the conversion of the ene groups. Nevertheless, since change in peak area of DM and DF occur on a similar timescale to the full conversion of allyl groups in DS, we expect thiol to preferentially react with allyl groups. Coupling this with Raman spectroscopy, where all vibrational modes are seen, we see a reduction in the ene peak of DM and DF over longer timescales, suggesting a slower chain growth background reaction consistent with the small molecule NMR studies. Since no homopolymerization occurs in DT3HD and thiol does add to the internal ene group, overall conversion of allyl groups is slower and limited.

RT FTIR Spectroscopy.

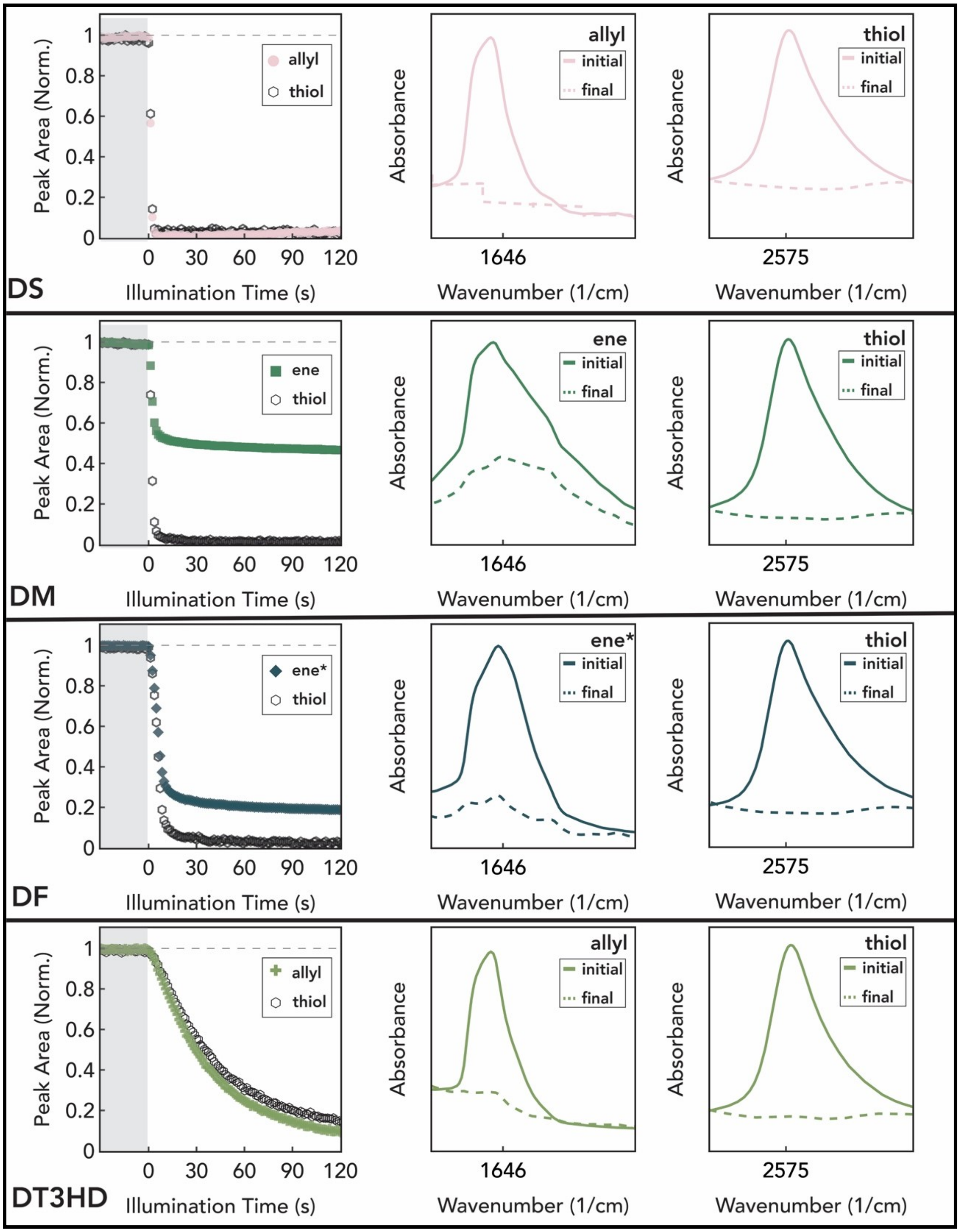

Figure S3-A1: Real-time FTIR spectroscopy monitoring conversion of (1) ene and thiol peaks, initial and final IR absorbance curves of (2) ene peak and (2) thiol peak during polymerization of TATO and ene monomer with **hexanedithiol** in 1:1 allyl:thiol ratio. *ene peak of DF only account for some vibrational modes of the fumarate group.

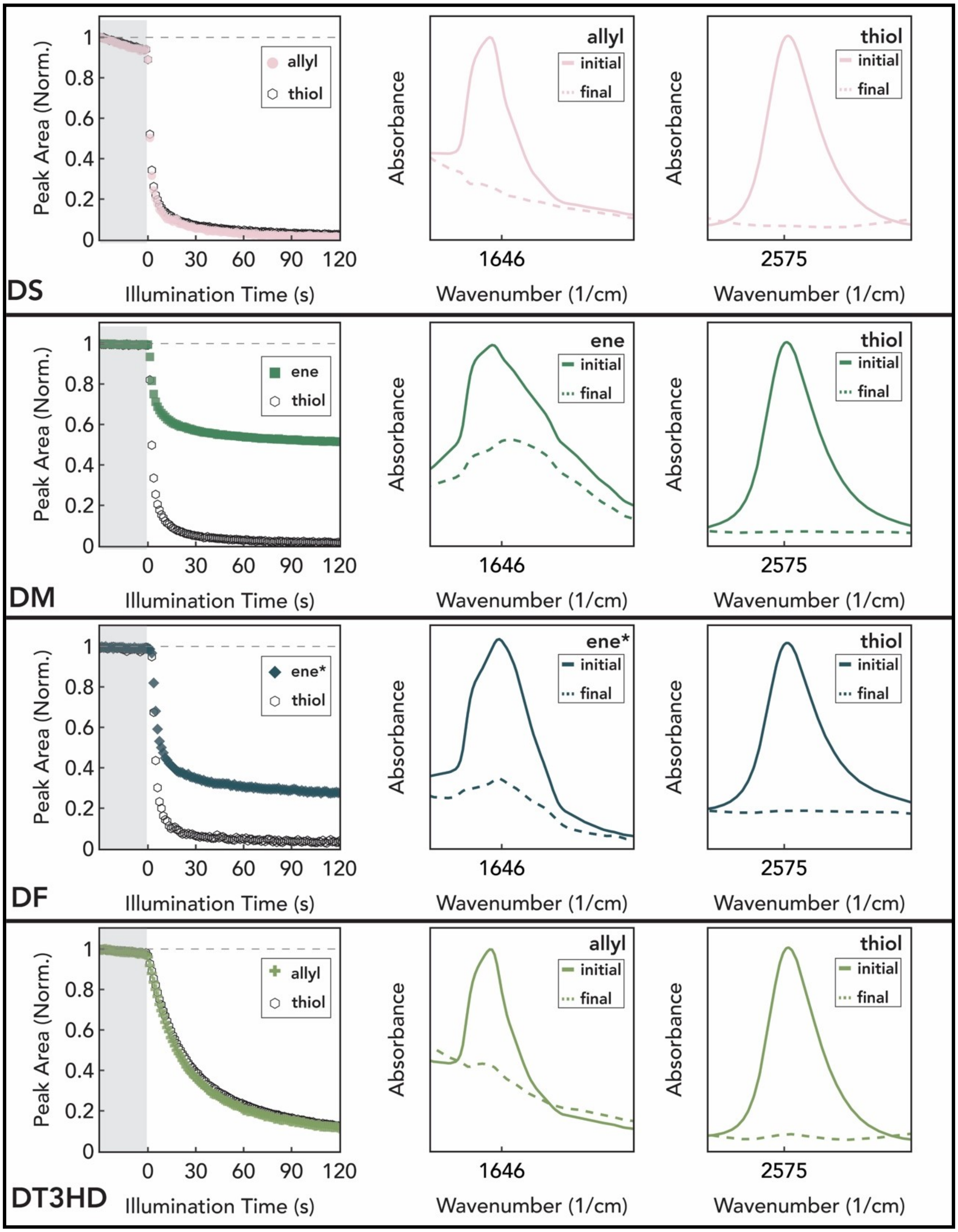

Figure S3-A2: Real-time FTIR spectroscopy monitoring conversion of (1) ene and thiol peaks, initial and final IR absorbance curves of (2) ene peak and (2) thiol peak during polymerization of TATO and ene monomer with **ethylene**

glycol bis(thioglycolate) in 1:1 allyl:thiol ratio. *ene peak of DF only account for some vibrational modes of the fumarate group.

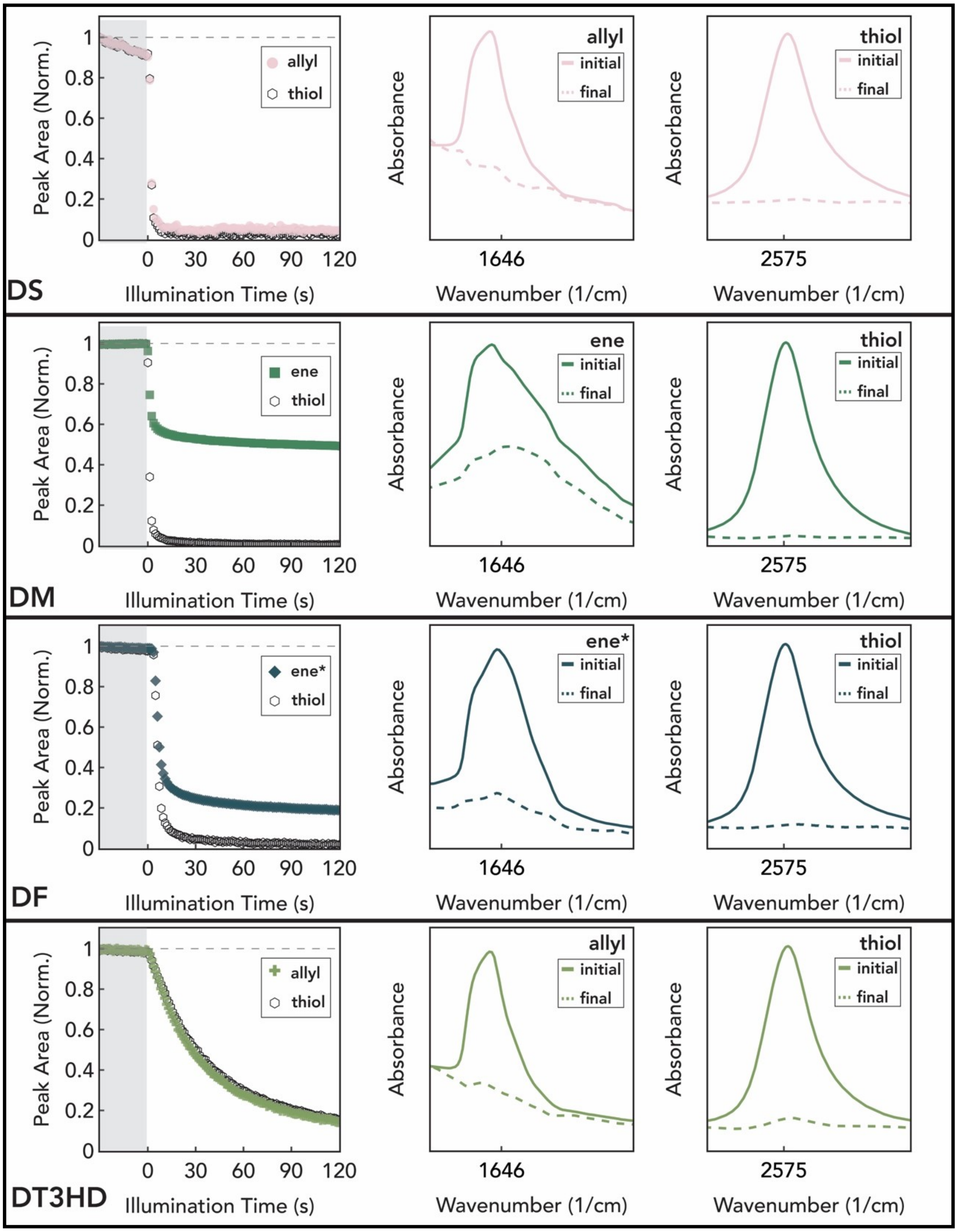

Figure S3-A3: Real-time FTIR spectroscopy monitoring conversion of (1) ene and thiol peaks, initial and final IR absorbance curves of (2) ene peak and (2) thiol peak during polymerization of TATO and ene monomer with **ethylene**

glycol bis(3-mercaptopropionate) in 1:1 allyl:thiol ratio. *ene peak of DF only account for some vibrational modes of the fumarate group.

Raman Spectroscopy.

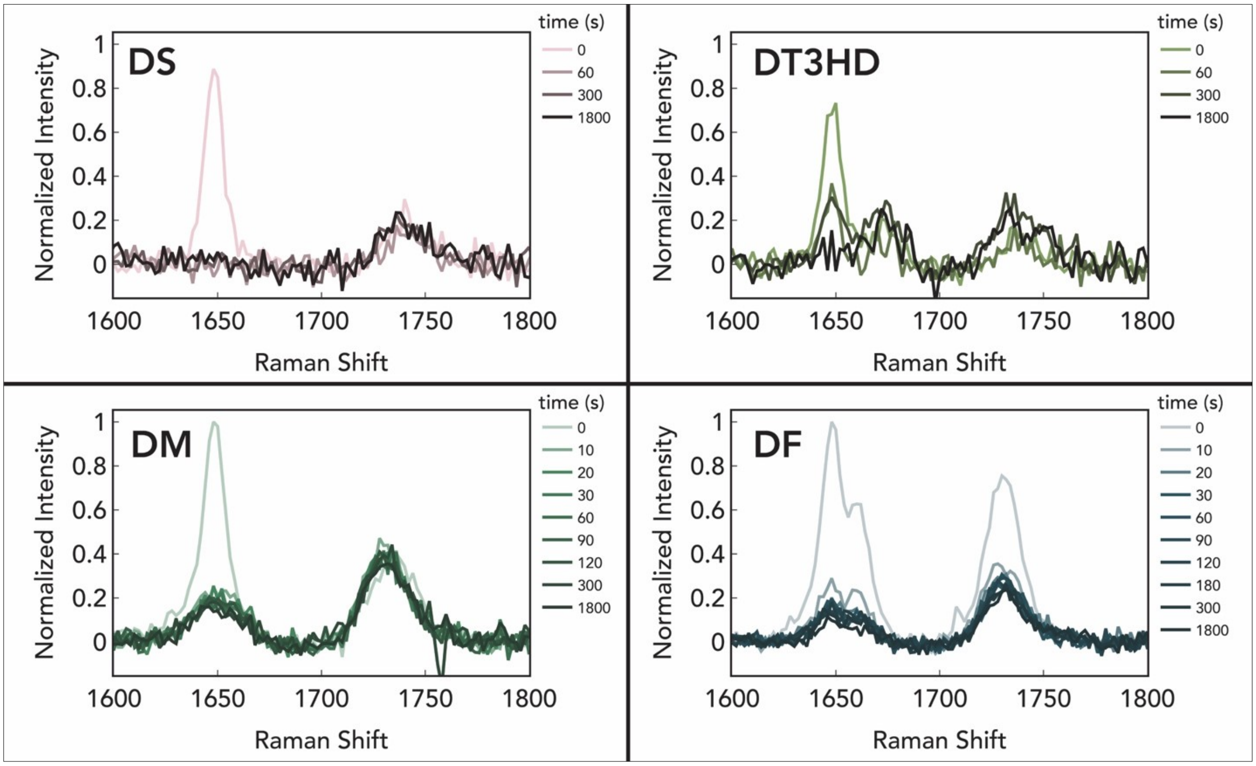

Figure S3-B1: Raman spectra monitoring conversion of ene peaks during photopolymerization of TATO and ene monomer with hexanedithiol.

Gelation by photo–rheology.

Mixed mechanism effects on network gelation were probed using photopolymerization. Systems with both reactivities (DM and DF) reached crossover point faster, thereby requiring much less energy for crossover, than DS and DT3HD. Further, in systems where crossover point is never reached with DS or DT3HD, it is reached with DM and DF (Fig S3-C2).

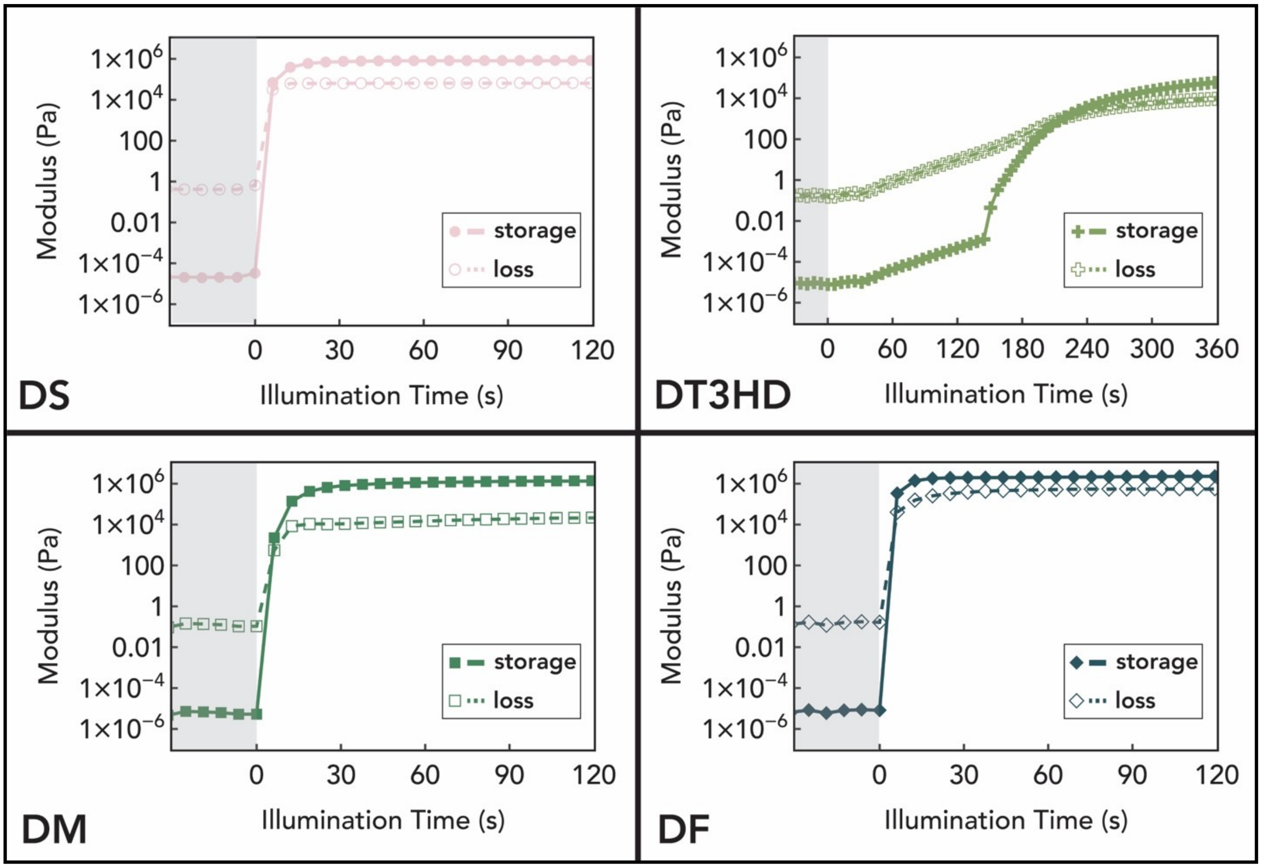

Figure S3-C1: Photo–rheology monitoring gelation of polymer networks during polymerization with **hexanedithiol** in 1:1 allyl:thiol ratio.

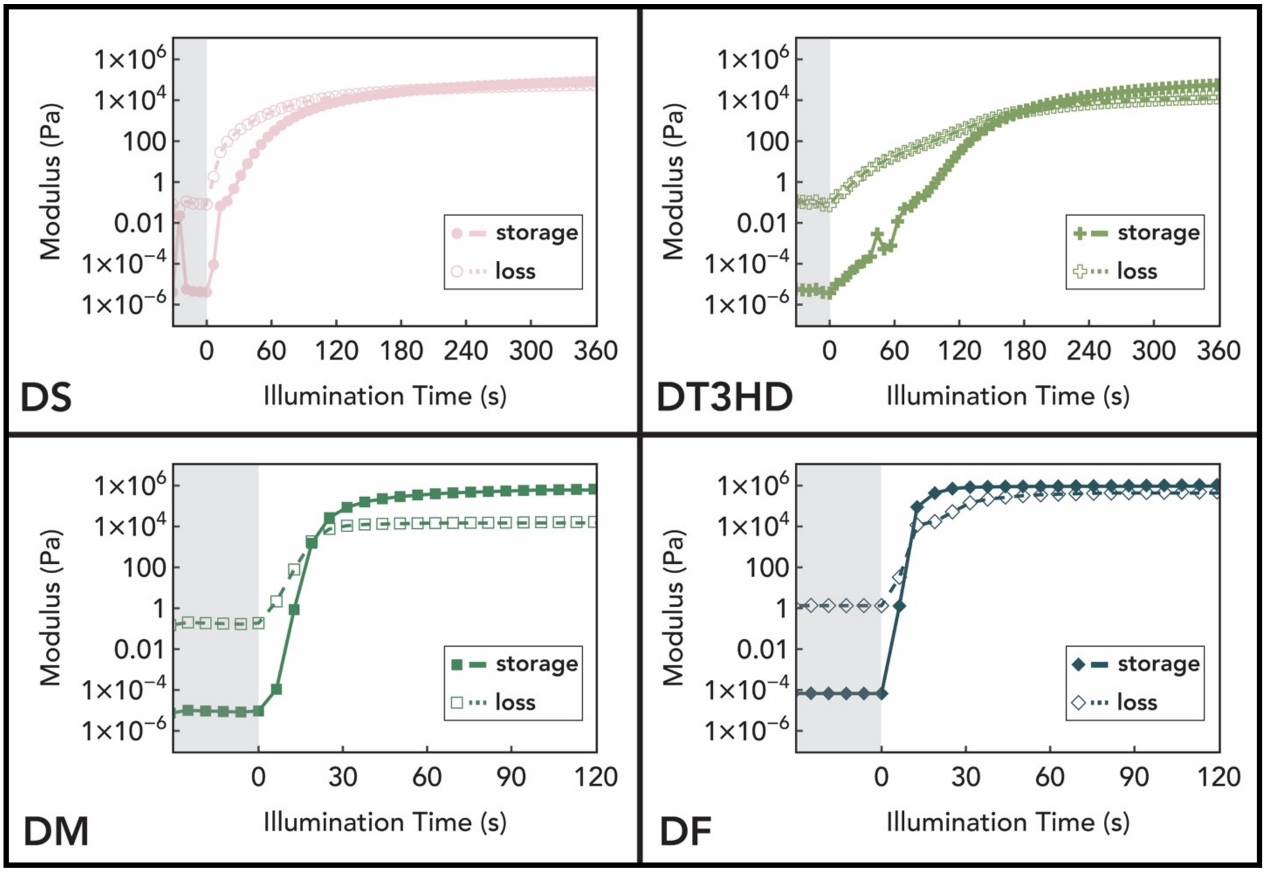

Figure S3-C2: Photo–rheology monitoring gelation of polymer networks during polymerization with **ethylene glycol bis(thioglycolate)** in 1:1 allyl:thiol ratio.

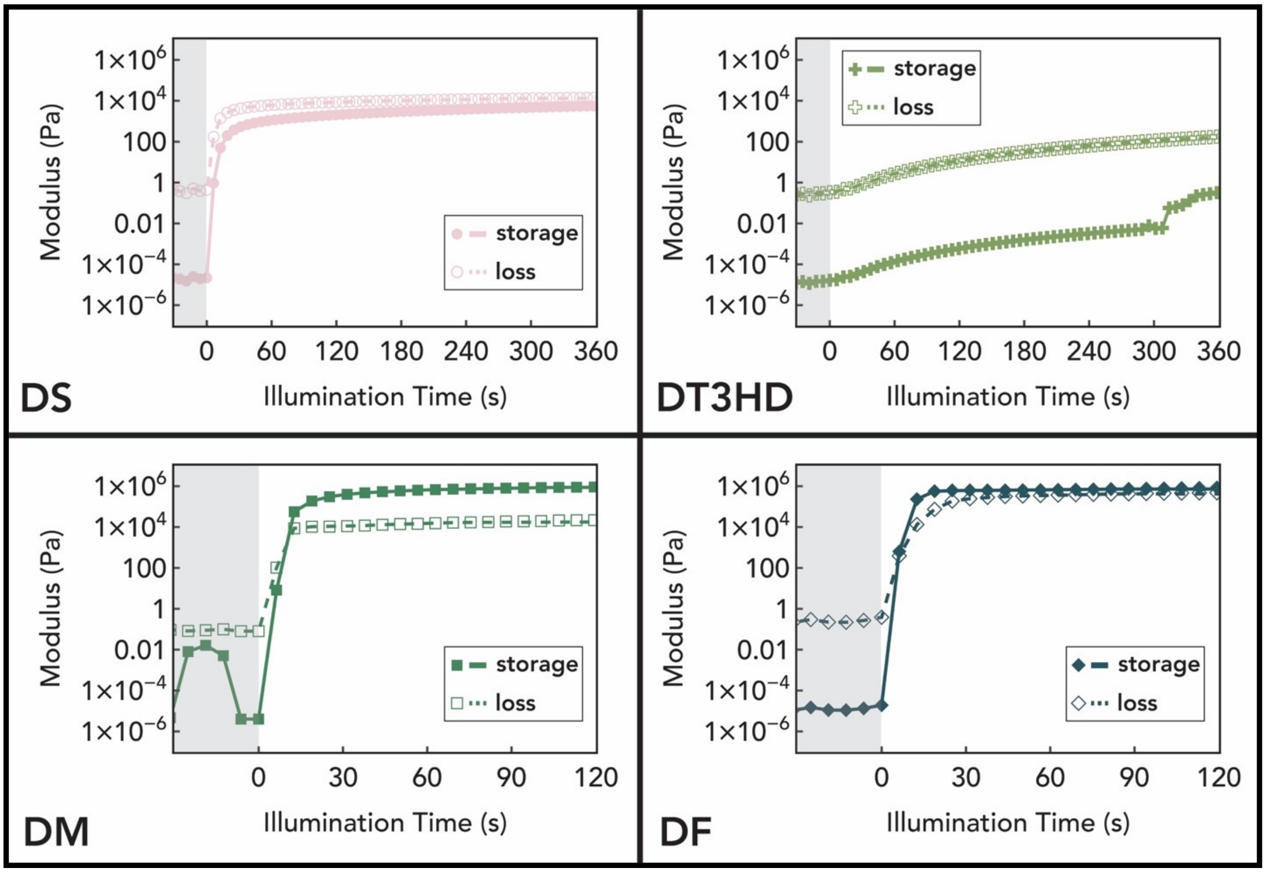

Figure S3-C3: Photo–rheology monitoring gelation of polymer networks during polymerization with **ethylene glycol bis(3-mercaptopropionate)** in 1:1 allyl:thiol ratio.

Mechanical Property Development.

Overview

Due to additional crosslinks forming from chain growth over longer illumination times, the molecular architecture of the polymer networks can be augmented. These differences in network topology can have large (up to a magnitude) impact on the mechanical properties of these polymeric materials within fully gelled networks.

Dynamic Mechanical Analysis.

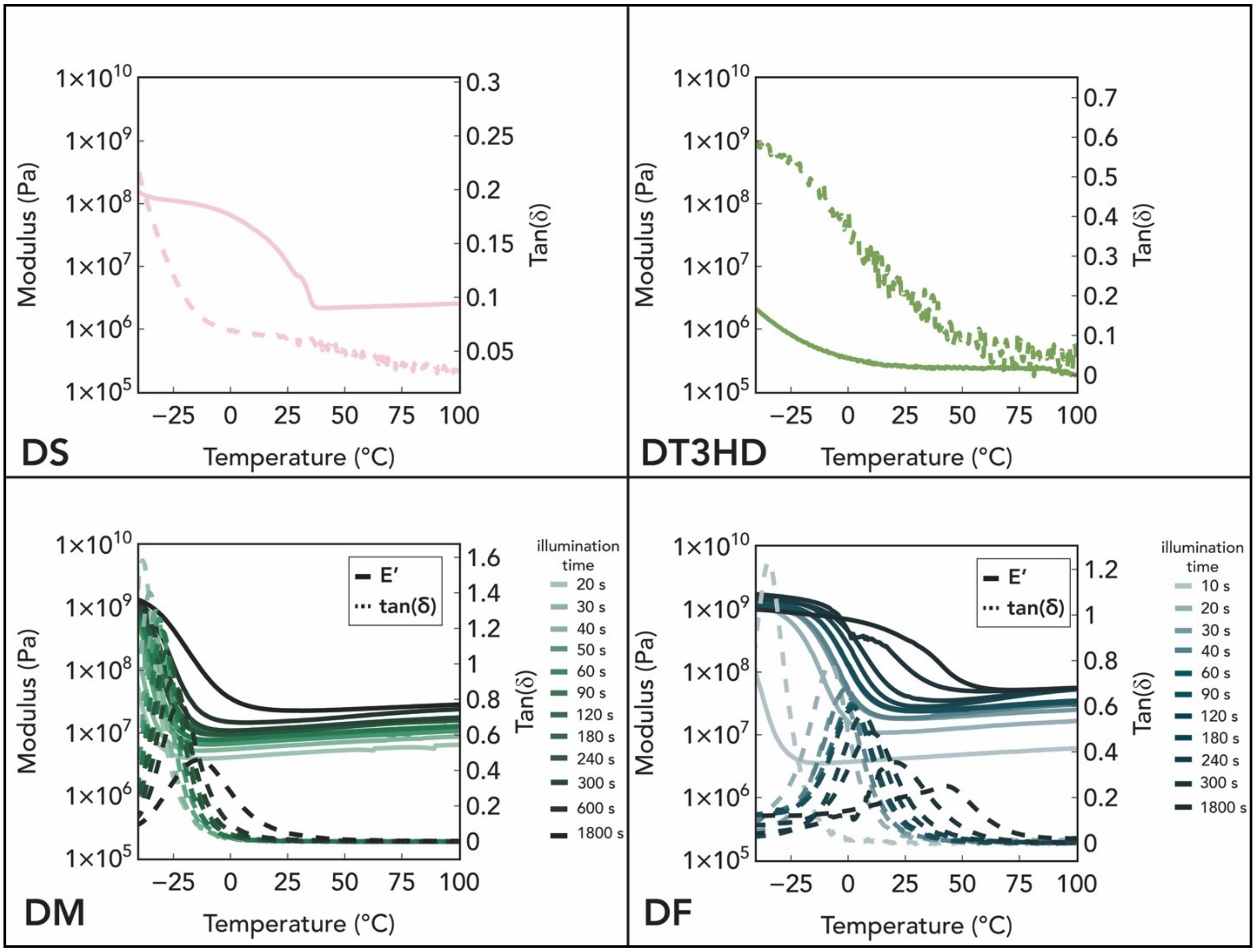

Figure S3-D1: DMA traces of polymer network films made with diallyl monomer, 5% TATO, and **hexanedithiol** in 1:1 allyl:thiol ratio. DF and DM showed changes in network structure over longer illumination times. Further, DS is shown to be crystalline at cold temperatures, which is suppressed in networks with maleic and fumaric moieties.

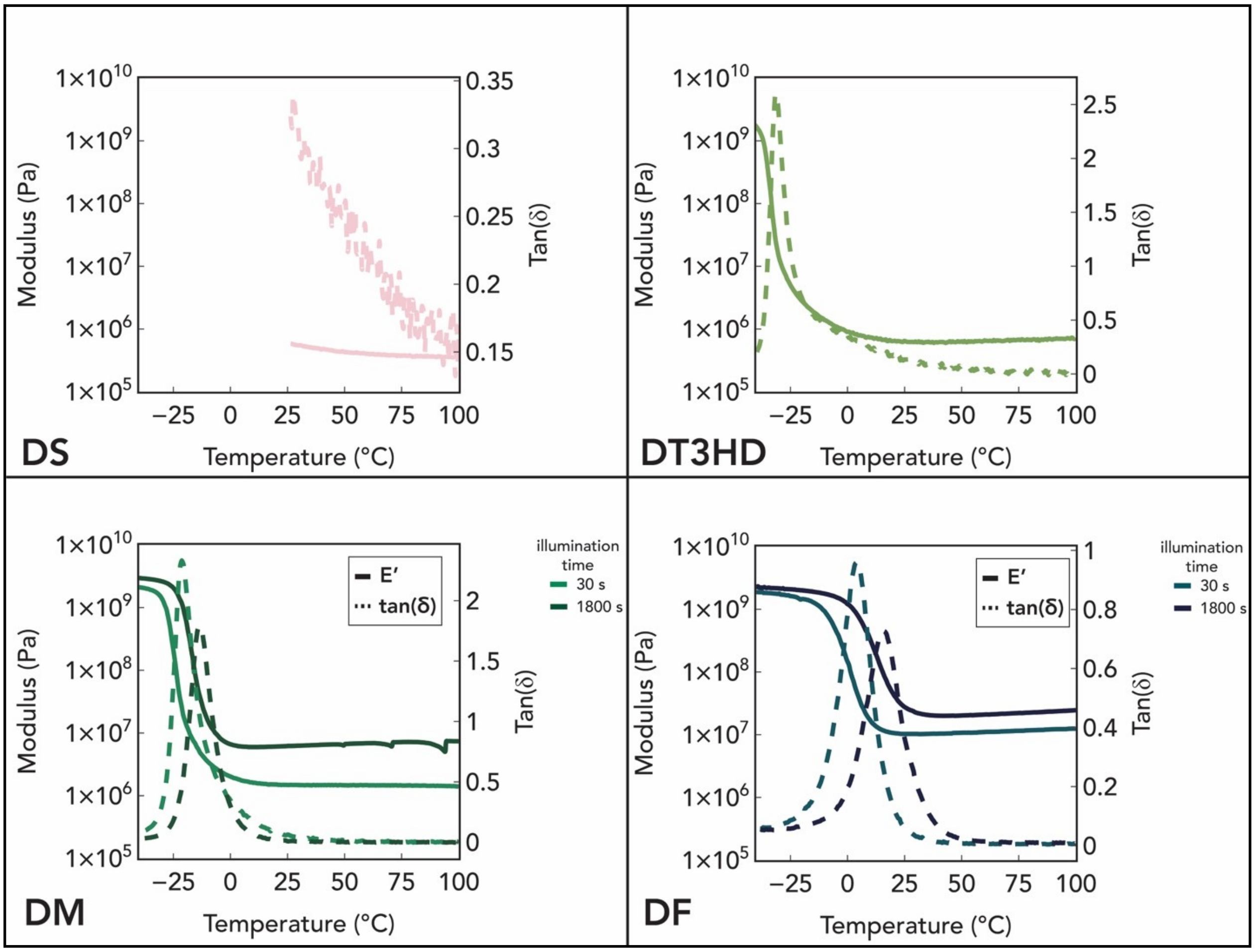

Figure S3-D2: DMA traces of polymer network films made with diallyl monomer, 5% TATO, and **ethylene glycol bis(thioglycolate)** in 1:1 allyl:thiol ratio. DF and DM showed changes in network structure over longer illumination times.

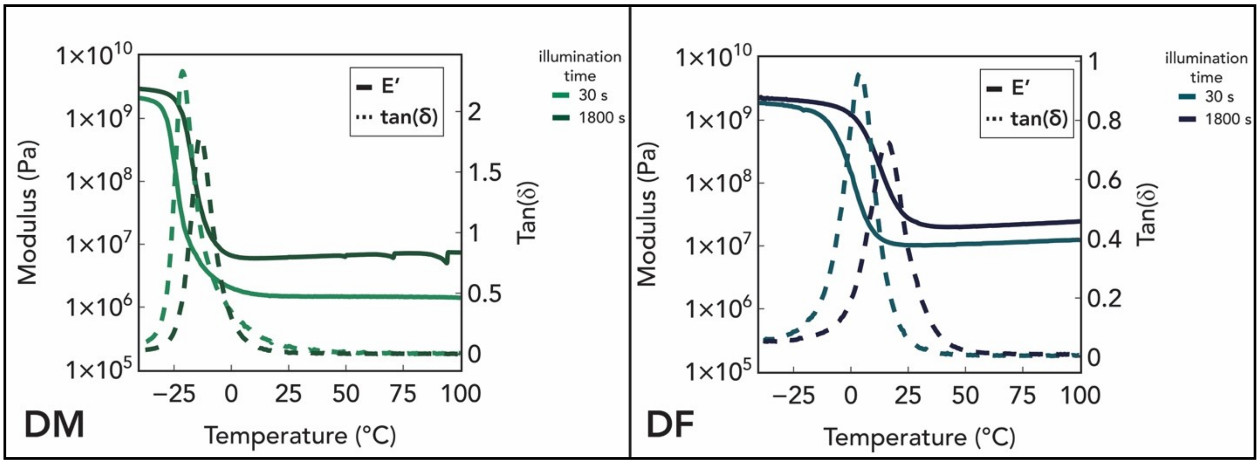

Figure S3-D3: DMA traces of polymer network films made with diallyl monomer, 5% TATO, and **ethylene glycol bis(3-mercaptopropionate)** in 1:1 allyl:thiol ratio. DF and DM showed changes in network structure over longer illumination times.

Heat Stability.

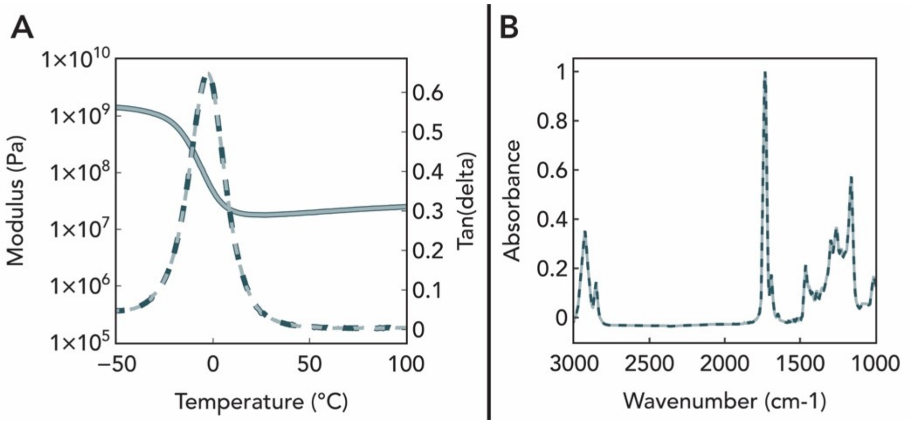

Figure S3-D4: There is negligible change before (light blue) and heating (dark blue) a specimen during heating at 100ºC for one hour. (A) Bulk mechanical properties by DMA show very similar properties before and after heating (B) FTIR spectra remains unchained before and after heating.

Gel Fractions.

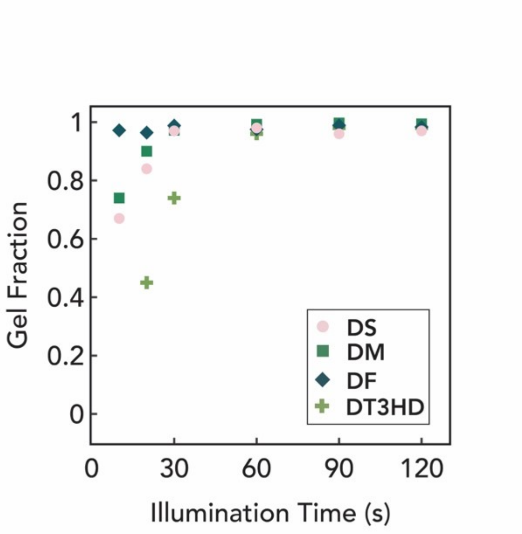

Figure S3-E1: Gel fractions of films made with hexanedithiol at varying illumination times.

4. Patterning Crosslinking and 3D Printing

Thin film photopatterning

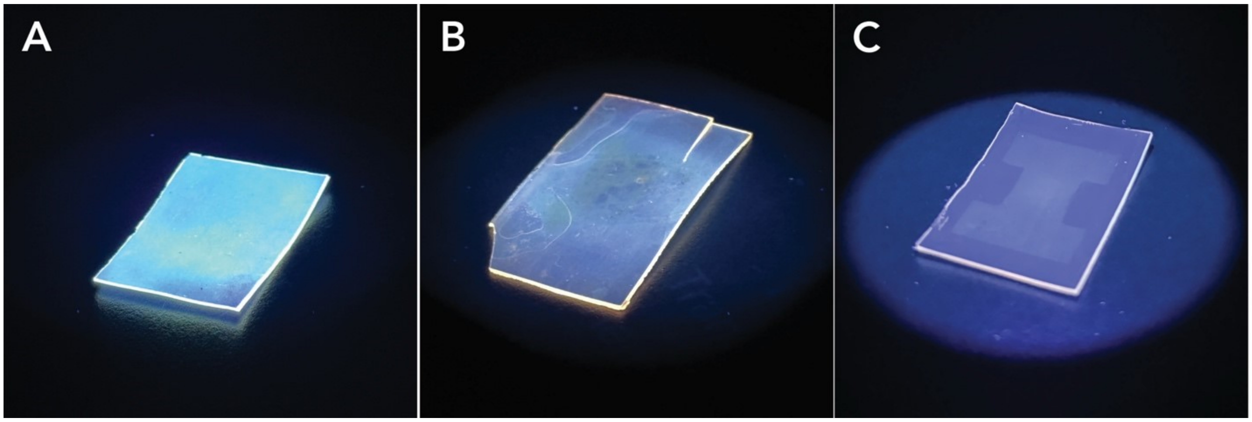

Figure S4-A1: Polymer networks formed using 5%TATO, diallyl monomer and hexanedithiol where UIUC's Block-I was photopatterned by forming an initial network polymer film under low light dose, placing a photomask on top, and illuminating the remaining film with additional light dose. These networks were subsequently swelled with fluorescent dye for visualization. **(A)**

DS film showed no I as expected and exhibited comparatively high fluorescence. **(B)** DM had low swelling differences between the two regions due to both regions remaining rubbery. **(C) D**F polymer film clearly depicts the block-I as the low exposed region is rubbery, while the highly exposed region is glassy – differentiating swelling ratios.

Vat photopolymerization additive manufacturing

Jacobs Working Curve.

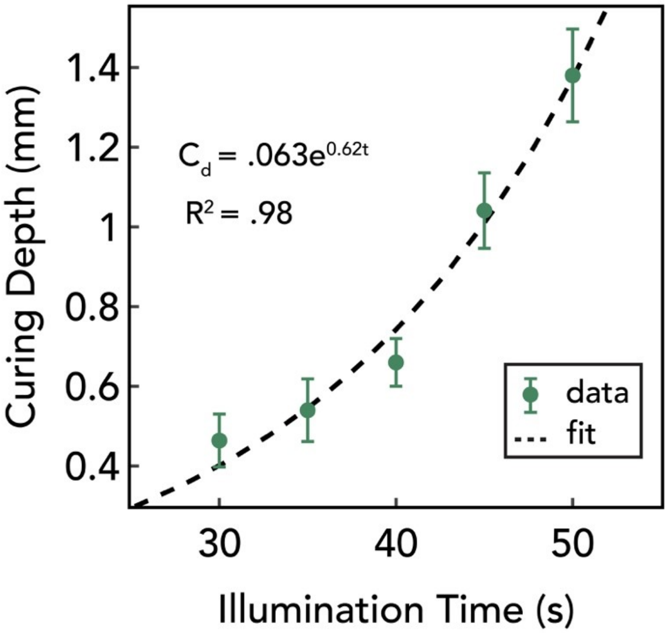

Figure S4-B1: Jacobs working curve for 5% TATO, diallyl maleate, hexanedithiol, with 0.01 wt% pyrogallol.

Additional prints.

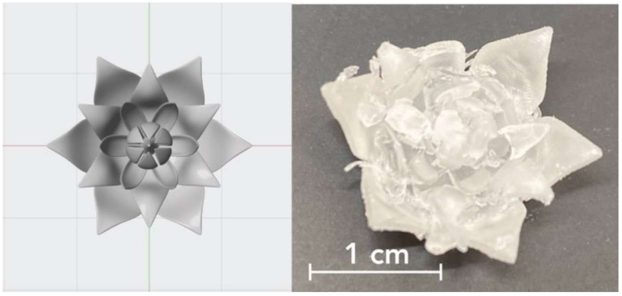

Figure S4-C1: 3D printed lotus flower using diallyl maleate, 5% TATO, and hexanedithiol as printing resin.

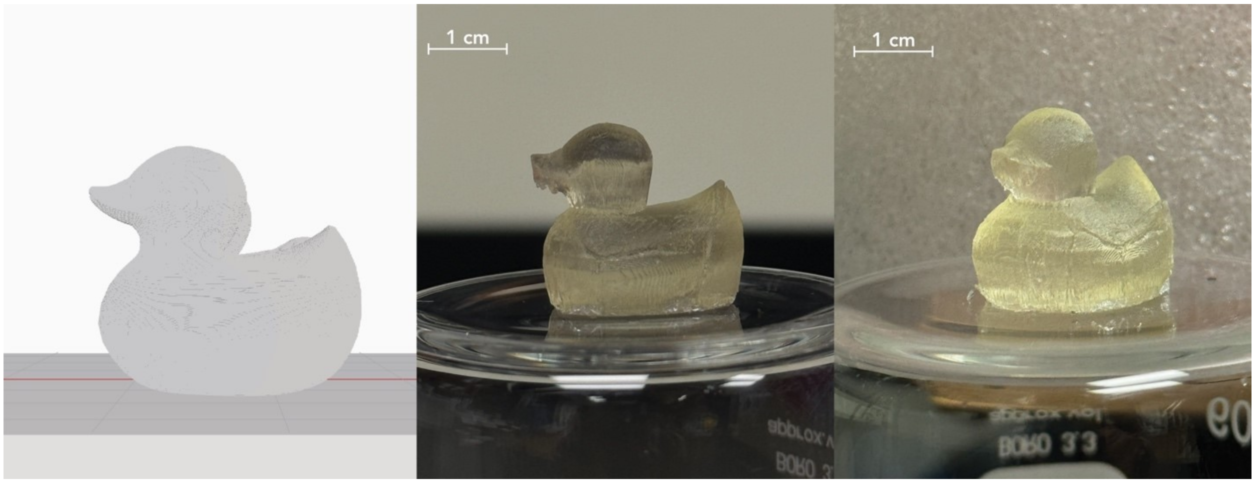

Figure S4-C2: 3D printed duck using diallyl maleate, 5% TATO, and hexanedithiol as printing resin.

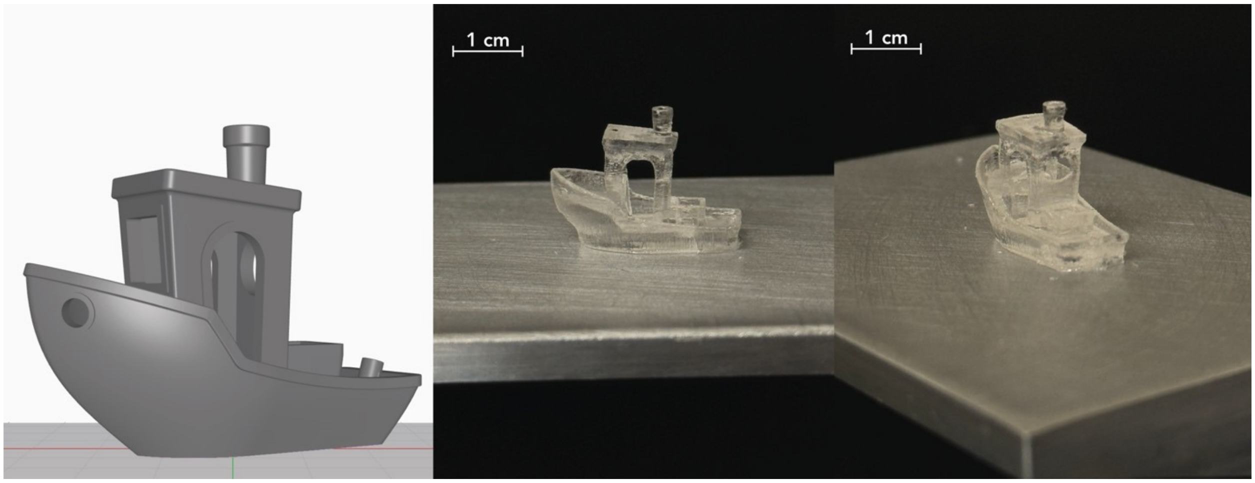

Figure S4-C3: Additional images of 3D printed 3D-Benchy using diallyl maleate, 5% TATO, and hexanedithiol as printing resin.

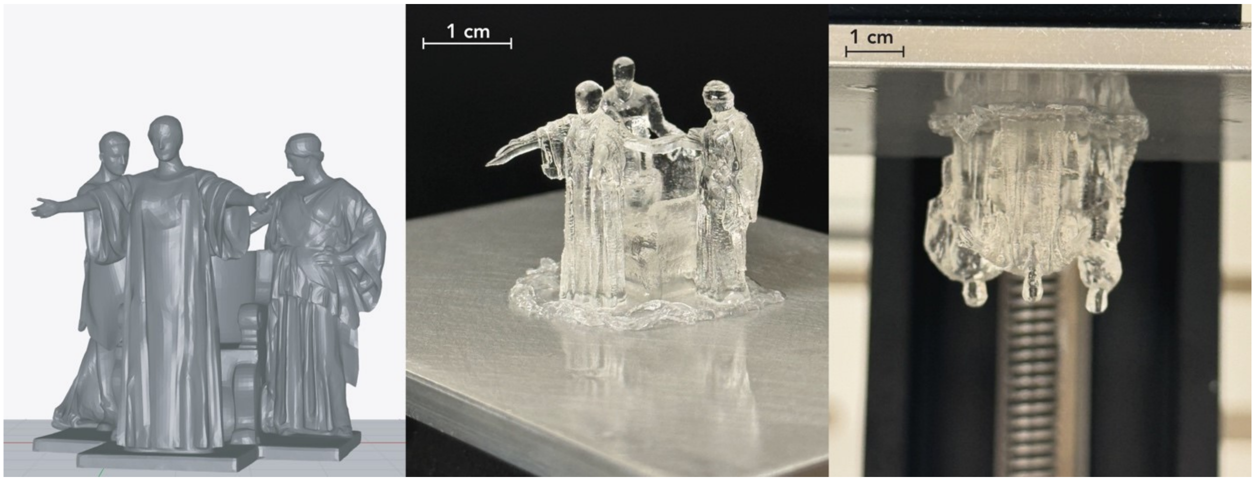

Figure S4-C4: Additional images of 3D printed Alma Mater statue of University of Illinois using diallyl maleate, 5% TATO, and hexanedithiol as printing resin.